

Impulse Radio Intrabody Communication System for Wireless Body Area Networks

Zibo Cai

College of Engineering and Science
Victoria University

Submitted in Fulfillment of the Requirements
For the Degree of
Master of Engineering (by Research)

Feb 2015

Abstract

Intrabody communications (IBC) is a novel physical layer outlined in the recently ratified IEEE 802.15.6 Wireless Body Area Network (WBAN) standard. This data communication method uses the human body itself as the signal propagation medium.

In this thesis, the limb joint effect for IBC signal transmission is investigated over a wider frequency range (0.3-200 MHz). The *in-vivo* measurement results show that the minimum signal attenuation points occur at 50 MHz and 150 MHz with average 2.0 dB signal path loss caused by the joint segments. In addition, the IBC channel attenuation characteristics are investigated on baseband digital signal transmission implemented on field programmable gate array (FPGA). A pulse position modulation (PPM) time division multiplexed (TDM) scheme was implemented for a baseband digital transmission. It was observed that the higher slot occupancy and pulse duty cycle provides lower signal attenuation.

Furthermore, an impulse radio (IR) transmitter was developed for galvanic coupling type IBC. IR transmitters typically have a simple structure in which the source data symbols modulate the pulses with a PPM scheme. The IBC transmission performance has been evaluated through a human arm experiment. Results demonstrate that there is 40 dB attenuation after 50 cm data transmission through human arm. The variations of the channel SNR is measured approximately 0.2 dB/cm for 5-50 cm on-body communication distances. The performance of proposed system has been showed based on theoretical simulation using bit error rate (BER) against signal propagation distance. The preliminary results of PPM baseband digital transmission characterization will improve the sensors network of the biomedical applications.

Student Declaration

Master by Research Declaration

“I, Zibo Cai, declare that the Master by Research thesis entitled [Impulse Radio Intrabody Communication System for Wireless Body Area Networks] is no more than 60,000 words in length including quotes and exclusive of tables, figures, appendices, bibliography, references and footnotes. This thesis contains no material that has been submitted previously, in whole or in part, for the award of any other academic degree or diploma. Except where otherwise indicated, this thesis is my own work”.

Signature:



Date: 12th, Feb, 2015

Acknowledgements

The most sincere and deep gratitude of mine should be given to my supervisor Dr. Daniel Lai, whose excellent supervision, professional guidance and encouragement have given me the strength and confidence necessary for the development of the study. In addition, I would like to thank Associate Pro. Francois Rivet for his positive and fruitful comments and research fellow Lance Linton for his support with empirical measurement.

I would like also to thank a most important colleague of mine, MirHojjat Seyedi, for his help during the research and his assistance in the experimental part of the work. Furthermore, I would like thank rest of my colleagues for their friendship, knowledge, and willingness to help. Many thanks also to the Research Group-Telecommunications, Electronics, Photonics and Sensors (TEPS) for the facility and financial support.

Overall, I would like to thank my family and my friends for their patience and support. I would also like to thank them for the care and advice that has always been helpful and much appreciated.

Zibo Cai
Melbourne, Feb 2015

List of Publications

Peer Review Conference Paper:

- Zibo Cai, MirHojjat Seyedi, Daniel T.H. Lai and Francois Rivet, "Characteristics of baseband digital signal transmission for intrabody communications," Instrumentation and Measurement Technology Conference (I2MTC) Proceedings, 2014 IEEE International , vol., no., pp.186,190, Uruguay, 12-15 May 2014.
- MirHojjat Seyedi, Zibo Cai, Daniel T.H. Lai and Francois Rivet, "An Energy-Efficient Pulse Position Modulation Transmitter for Galvanic Intrabody Communications," International Conference on Wireless Mobile Communication and Healthcare, vol., no., pp.192,195, Greece, 3-5 Nov. 2014.

Peer Review Journal Paper:

- MirHojjat Seyedi, Zibo Cai and Daniel T.H. Lai, "Characterization of Signal Propagation through Limb Joints for Intrabody Communication," *International Journal of Biomaterials Research and Engineering (IJBRE)*, vol. 2, pp. 1-12, 2013.

Contents

Abstract	II
Student Declaration	III
Acknowledgements	IV
List of Publications	V
Contents	VI
List of Figures	VIII
List of Tables	XI
Chapter 1 Introduction.....	1
1.1 Biomedical monitoring.....	2
1.2 Wireless Body Area Network (WBAN).....	4
1.3 Human body communications (HBC)	7
1.4 Research objectives	10
1.5. Outline of the Thesis.....	11
Chapter 2 Background	13
2.1 Digital communication systems	14
2.1.1 Shannon sampling theorem	14
2.1.2 Multiplexing	16
2.1.3 Modulation scheme	17
2.2 IBC transmission system	20
2.2.1 Baseband communication system	21
2.2.2 IBC coupling methods	22
2.2.3 Current IBC communication systems	24
2.3 Conclusion.....	28
Chapter 3 Limb Joints Effect.....	30
3.1 Methodology	31
3.1.1 The preparation for measurement	32
3.1.2 Measurement system design	32
3.1.3 Test protocol.....	34

3.2 Experiment setup	35
3.3 Measurement Results	39
3.4 Discussion	46
3.5 Conclusion.....	48
Chapter 4 Effect of user occupancy with baseband PPM.....	49
4.1 Experiment setup	50
4.2 Results and discussion.....	53
4.2.1 Pulse Duty Cycle.....	53
4.2.2 Pulse Occupancy for Fixed Timeslot Duration.....	55
4.2.3 Pulse Occupancy for Increasing Timeslot Duration	57
4.3 Conclusion.....	59
Chapter 5 Characterization of IBC System.....	60
5.1 PPM modulation scheme	60
5.2 IBC System Design.....	63
5.3 Experiment setup	65
5.4 Results and discussion.....	67
5.4.1 IBC signals (Time and Frequency domain)	67
5.4.2 Path loss characteristics.....	70
5.4.3 Signal propagation noise	72
5.4.4 Communication performance.....	75
5.4.5 BER evaluation	76
5.5 Conclusion.....	78
Chapter 6 Conclusions and Future Work.....	80
6.1 Thesis Summary	81
6.2 Challenges	82
6.3 Future work	83
References.....	85

List of Figures

Fig. 1.1 Sensor network of biomedical monitoring application	2
Fig. 1.2 The cooperation of WBAN with other kinds of wireless networks	4
Fig. 1.3 Targeted position of BAN among other popular wireless networks	6
Fig. 1.4 IEEE 802.15.6 base architecture	7
Fig. 2.1 Basic elements of a digital communication system	14
Fig. 2.2 Channel capacity against bandwidth for channels under AWGN	15
Fig. 2.3 Symbol structures for OOK and 4-PPM	19
Fig. 2.4 Simplified block diagram of the IBC transceiver system	20
Fig. 2.5 Simplified block diagram of the (a) passband system and (b) baseband system	21
Fig. 2.6 Capacitive coupling and galvanic coupling for data transmission between transmitter and receiver units	22
Fig. 3.1 The schematic diagram of the employed balun in the measurement setup	33
Fig. 3.2 The balun loss at desired frequency range of this study ..	34
Fig. 3.3 Variation of human tissues electrical properties, relative permittivity and conductivity, against frequency [33]	35
Fig. 3.4 The measurement setup of the IBC technique	37
Fig. 3.5 Source transmitter waveform (50 MHz) measured by oscilloscope using IBC method	38
Fig. 3.6 The signal attenuation of the arm for 0.3-200 MHz	40
Fig. 3.7 IBC received signal and fast Fourier transform (FFT) in 50 MHz (a) female (b) male test subject	43
Fig. 3.8 Received signal and fast Fourier transform (FFT) in 150 MHz (a) female (b) male test subject	45

Fig. 4.1 The measurement setup using Pulse Generator and Oscilloscope (method a)	51
Fig. 4.2 The measurement setup of FPGA board and oscilloscope (method b).....	52
Fig. 4.3 The signal attenuation of the body channel for input signal with 20%-50% duty cycle when Data Generator was used as transmitter	53
Fig. 4.4 The attenuation of signal propagated in different duty cycles generated by FPGA board	55
Fig. 4.5 The transmitted signal in 1, 3, 5, and 7 timeslots occupied	56
Fig. 4.6 The signal attenuation of both male and female subject forearm in 1-7 timeslots occupied using FPGA implementation	57
Fig. 4.7 Sample of a digital wave at 1-3 timeslots at pulse frequency of 12.5 MHz.....	57
Fig. 4.8 The signal attenuation of the body forearm for 5.0-25.0 MHz in 1 to 3 timeslots occupied using FPGA implementation.....	58
Fig. 5.1 Diagram of L=4 PPM	62
Fig. 5.2 A simplified architecture of the IBC PPM transmitter	63
Fig. 5.3 The 4 and 8 PPM transmitter output pattern	64
Fig. 5.4 The measurement setup and protocol of galvanic coupling IBC using FPGA board, transmitter.....	66
Fig. 5.5 Waveform of 4 PPM transmitter output.....	67
Fig. 5.6 The detected 4 PPM signal from on-body electrodes	67
Fig. 5.7 The output signals of 4 and 8 PPM IBC transmitter (Tx) at 0-25 MHz range.....	68
Fig. 5.8 The comparison of IBC signals spectrum, IBC transmitter (Tx) output before body and IBC receiver (Rx) output after propagating through body for (a) 4 PPM and (b) 8 PPM at 25 MHz range	69
Fig. 5.9 Path loss vs distance characteristic for IBC.....	71
Fig. 5.10 The received signal with 10cm, 15cm, 25cm and 45cm (Tx-Rx) distance.....	73

Fig. 5.11 The amplitude of IBC received signal and noise using (a) 4 PPM modulation scheme and (b) 8 PPM between 5.0 and 50 cm at human arm channel at subject-1.....	73
Fig. 5.12 The analytical model of the human body communication channel during different on-body channel length	74
Fig. 5.13 The SNR versus channel length or distance (5-50 cm) using 4 and 8 PPM IBC system for both subject-1 and subject-2	75
Fig. 5.14 The simulation result of BER versus distance for 4 and 8 PPM	78

List of Tables

TABLE 1.1. The technical requirements of body area network sensor nodes	3
TABLE 1.2 Characteristic of Common RF technologies used in WBAN	7
TABLE 2.1 Summary and comparison of current IBC communication system	28
TABLE 3.1 The signal characteristics of male subject body during IBC	39
TABLE 4.1 The propagated signal characteristics at 50 MHz using pulse generator	54
TABLE 4.2 The signal characteristics of body at 25 MHz.....	59
TABLE 5.1 Mapping of 2 bits and 3 bits words into 4 and 8 PPM symbols	62

Chapter 1

Introduction

Personal health monitoring is increasingly important to detail the changes of our health status. A study shows that 40% of patient care time is used for health reporting requirements. By 2020, USA will lack over 1 million nurses. More and more hospital beds need next generation patient monitoring devices [1] which could reduce costs for patients and national healthcare systems. Such rapidly increasing personal healthcare requirements highlight the urgent need for new technology with low cost and affordable solutions for human life quality improvement. Currently, the primary focus of technological development is on various healthcare measurement instruments and monitoring devices, which aim to improve the quality of healthcare monitoring. There is a huge demand for low-power, low-cost, wireless sensors in the medical field. In addition, interest in remote monitoring technologies and electronic medical records is exponentially increasing.

Health monitoring will soon become a major necessity for a better quality of life. A new emerging paradigm is the use of networked sensors to monitor health, in a framework known as healthcare sensor networks [2]. These healthcare sensor networks will contribute to global healthcare systems by application of high and low frequency signal propagation using ultra-low power for maximizing monitoring time. Since the connection between most existing sensors and medical monitors is not wireless, the future monitoring platform looks set to replace the data cables with wireless communication links to improve portability. During the last four years, 7.5 million households in the U.S are using wireless communications technology [3]. The wireless health monitoring system is set to benefit medical care with its convenience, easy installation and low cost.

1.1 Biomedical monitoring

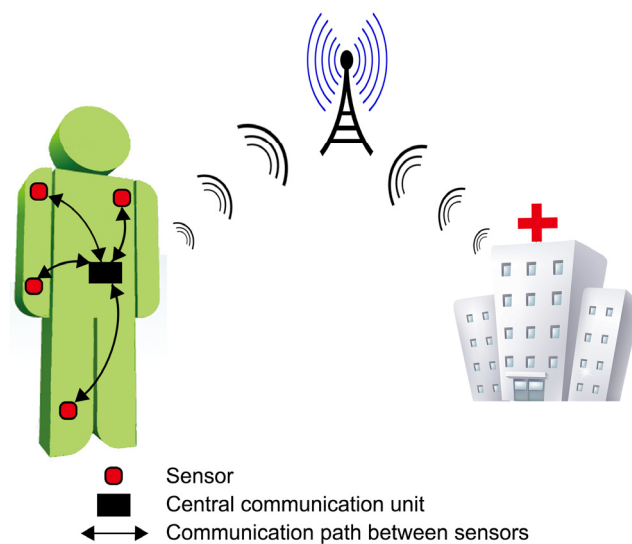


Fig. 1.1 Sensor network of biomedical monitoring application

CHAPTER 1. INTRODUCTION

For health monitoring, data acquisition and correct signal recording are the most fundamental requirements. In the hospital, biomedical sensors attached to different parts of human body are used to monitor patient vital signs such as body motion, body temperature, blood pressure, blood glucose levels, using techniques such as e.g. electrocardiogram (ECG), electroencephalography (EEG), pulse oximetry (SpO₂). A network should be built for the communication path between those sensors. Fig.1.1 shows an example sensor network of biomedical monitoring applications [4]. The network of sensors is much more energy efficient and portable if the data communication between sensors is wireless. A new wireless sensor network should be created for providing higher data resolution and lower power consumption. The wireless sensors send the physiological data through the human body to the central communication unit. After that, the patient's data is communicated the hospital access terminal. The physical activity of patient is monitored by the biomedical monitoring system, which is online and real-time. Due to energy efficiency, the duty cycle of body area network signal is around 1-10% as the purpose of continuous data streaming. Further, there various sensors with 1-10% duty cycles resulting in larger occupancy of communication channel. TABLE 1.1 presents the technical requirements of body area network sensor nodes [5].

TABLE 1.1. The technical requirements of body area network sensor nodes

Application	Data rate	BER	Duty cycle
ECG	72kbps	<E -10	<10%
EMG	576kbps	<E -10	<10%
O ₂ /temp/glucose monitoring	10kbps	<E -10	<1%

1.2 Wireless Body Area Network (WBAN)

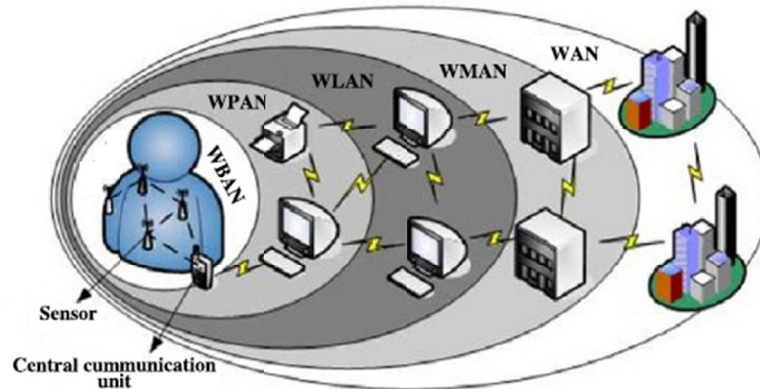


Fig. 1.2 The cooperation of WBAN with other kinds of wireless networks . Reproduced from [6]

It should be noticed that the development focus of communication networks is shifting from wide area network (WAN) to wireless metropolitan area network (WMAN), and then, to wireless local area network (WLAN), after that, to wireless personal area network (WPAN), eventually now, to wireless body area network (WBAN) (see Fig. 1.2). WAN is a computer network connection using microwaves, radio waves or coaxial cable. WMAN and WLAN are connecting computers in a city or in an office building respectively. WPAN is a wireless network for device connections in an individual person's workspace. It usually refers to the communication between the wearable device and off-body base units. WBAN is a wireless network for human body communication implementation consisting of miniature sensors worn on the body, communicating with an on-body based unit.

WBAN is becoming increasingly popular in health monitoring, sports and the personal entertainment area. The WBAN technology is the use of wireless communications between sensors and central communication unit. The WBAN consists of central

CHAPTER 1. INTRODUCTION

communication unit and several sensors. Those sensors send physiological data to the central communication unit. The human-centric operation of WBAN leads to unique research issues for sensor network technology, particularly how to reduce power consumption while improving the data rate with efficient pulse duty cycle (i.e. energy efficient system design). The idea of WBAN could prove to be a major solution in healthcare as the telemedicine and patient monitoring or other applications including the field of sports, security and defence.

The wireless connectivity among devices placed around the human body is the key technology for health monitoring in the hospital or at home. The sensor networks required the new physical layer which involves the actual signal transmission and reception over the human body channel. The IEEE 802.15 task groups are the physical layers defined for the development of a standard for WLAN, WPAN and WBAN. IEEE 802.15 includes seven different task groups [7]:

- IEEE 802.15.1 is a WPAN standard based on the Bluetooth specifications.
- IEEE 802.15.2 addresses the WPANs operating in unlicensed frequency range such as WLAN.
- IEEE 802.15.3 develops a standard for high-rate (11 to 55 Mbit/s) communications.
- IEEE 802.15.4 provides low data rates and complexity, long term battery life (months). It is based on ZigBee technology.
- IEEE 802.15.5 is for the specification of networking for WPAN.
- IEEE 802.15.6 focused on WBAN technologies. It aims an energy efficiency and short distance wireless standard.
- IEEE 802.15.7 writes a standard for Visible Light Communications (VLC).

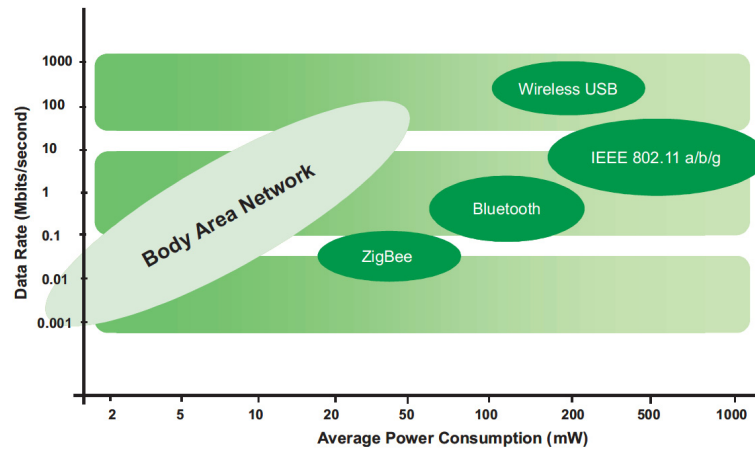


Fig. 1.3 Targeted position of BAN among other popular wireless networks

IEEE 802.15.6 (WBAN standard) combines medical, lifestyle and entertainment applications and was officially published in early 2012. Fig.1.3 shows the targeted position of BAN among other popular wireless networks [8].

There are several candidates for the wireless connectivity in WBAN. As the first family standard of IEEE 802.15, Bluetooth is a point-to-point or point-to-multi-point data transmission system. It operates in the 2.4 GHz industrial scientific and medical (ISM) band and occupies 79 channels. The primary modulation method is phase shift keying (PSK). Bluetooth mainly supports voice links, but suffers from higher power consumption (see table 1.2). The classical Bluetooth could achieve approximately 1Mbps data rate with power consumption about 150 mW during human body communication. [9].

ZigBee technology is a protocol with low power consumption and low data rate for wireless network. Long battery life (years) equipment needs is fulfilled by ZigBee which provides low cost and low power. Zigbee is optimized for industrial sensor

TABLE 1.2 Characteristic of Common RF technologies used in WBAN

Technology	Frequency [GHz]	Data rate [bit/s]	Power consumption [mw]
WLAN (IEEE 802.11a/g/n)	2.4-5.1	54M	100mW
Bluetooth (IEEE 802.15.1)	2.4	1-24M	10mW
Zigbee (IEEE 802.15.4)	2.4	250k	1mW

application, but it has a huge disadvantage of low data rate, for instance, 1 byte transmitted every 5 minutes [10]. TABLE 1.2 shows the characteristic of WLAN, Bluetooth and Zigbee technologies used in WBAN.

1.3 Human body communications (HBC)

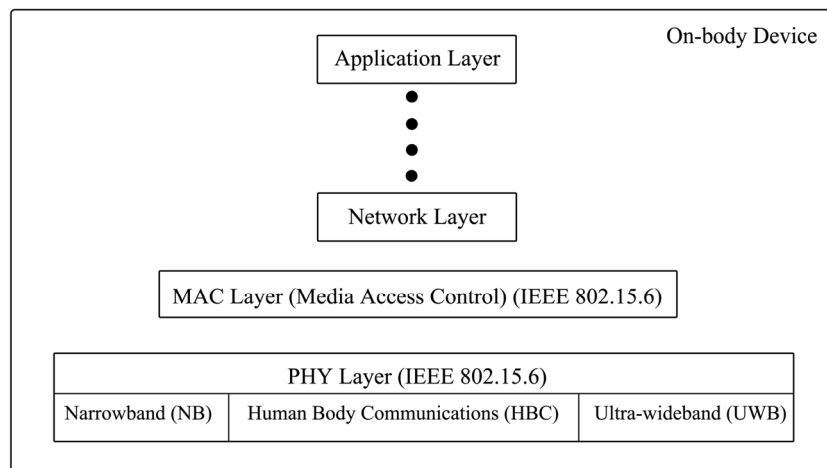


Fig. 1.4 IEEE 802.15.6 base architecture

CHAPTER 1. INTRODUCTION

Wireless monitoring devices present a revolutionary change in healthcare applications by means of portable devices. Radio frequency (RF) technology is one of the suitable choices in the development of portable devices. However, the RF spectrum is overcrowded because every radio technology allocates a specific part of the spectrum (ISM band). WBAN technology offers minimal interference than current radio system with whilst avoiding the expensive spectrum licensing fees. It promises to be a great potential revolution of the healthcare technology in the future [11]. The purpose of the recently ratified IEEE 802.15.6 by the Federal Communication Commission (FCC) is to define new wireless standards Physical (PHY) and Medium Access Control (MAC) layers for WBAN. The IEEE 802.15 Task Group 6 defines a MAC layer and a few supporting PHY layers for Body Area Networks (BAN) application in, on, or around a human body. IEEE 802.15.6 determines three PHYs, named Narrow Band (NB), Ultra Wide Band (UWB) and Human Body Communication (HBC) (see Fig. 1.4) [12]. The first two are radio frequency (RF) techniques; the last one is a new non-RF communication method using human body tissue as a transmission medium [13].

All the three PHYs are defined for different system demands and target applications. The NB and UWB provide a high data rate with low power consumption. However, the frequency band of NB located in three different unlicensed bands (402-409 MHz for implantable application, 863-956 MHz for wearable devices and 2.36-2.4 GHz for medical needs) is noisy and interfered by WiFi, Bluetooth and Zigbee. UWB PHY operates in three frequency bands: high band (between 6 and 10.6 GHz), low band (from 3.1 to 4.8 GHz) and sub-GHz band (from 0 to 960 MHz). These bands of UWB suffer from huge signal propagation loss through the human body due to body shadowing effects (more than 60 dB [14]) which cause high power consumption of WBAN devices. The UWB and NB communication have another disadvantage

CHAPTER 1. INTRODUCTION

regarding path loss (40-100 dB [15]) compared with HBC due to higher human body conductivity with electrode interface than air channel with antenna interface. Therefore, HBC PHY has advantage over NB and UWB PHY and promises to be a suitable candidate for WBAN application.

HBC is a new wireless communication technique based on signal propagation through the human body. In this method human body acts as conductor to transmit all or a major portion of data between sensors and central communication unit that are attached on or implanted in the body. Furthermore, it eliminates connecting cable and wireless antenna from biomedical monitoring communication devices. This short-range wireless communication technology for WBAN provides wearable sensors and implanted devices with an alternate solution to RF communications. The development of the HBC will provide less complexity and convenient communication network for these electronic devices. The advantage of natural security attached to the HBC due to the physical contact of transmitter and receiver node vastly outweighs the RF communication techniques.

Normally, HBC works under 100MHz and 21MHz is the center frequency of its operation band [13]. HBC has been cited by other papers as body channel communication (BBC) [16] or intrabody communications (IBC) [16]. According to [17], intrabody communication is a novel data propagation method using the human body as the transmission medium for electrical signals. Due to outside coverage of the IEEE 802.15.6 standard, IBC has been used to stand for this transmission approaches in this thesis. The characteristics of the IBC technique are as below.

Body shadowing: Unlike RF technologies (IEEE 802.15.4), IBC does not suffer from body shadowing [18].

Path loss: Compared with air channel, IBC uses human biological tissues as communication channel; it has lower propagation loss because of higher conductivity of the human body as well as lower environmental noise and interference [19].

Security: It is safe for human being, because lower frequency leads to lower radiation. It is a reliable communication method because of lower interference inside human body and lower radiation to the outside of human body [20]. Additionally, lower voltages and currents are used in transceivers.

Power consumption: Lower frequency than RF and no analog front-ends block requirement lead to lower power consumption. Low power density contributes to less electromagnetic energy absorption in human body [19].

The human-centric WBAN operation needs to take the technical hardware requirements into account. Instead of low impedance antennae, other electrodes can be used for lowering the frequency of communication link, and then reducing power consumption of IBC transceivers. This raises research issues concerning transceiver circuit design, as a fundamental stage of WBAN system, particularly reducing power consumption while improving the data rate. This research will contribute towards the development of improved low power human IBC technologies for WBAN.

1.4 Research objectives

IBC is a low-frequency technology leading to a future generation of short-range communication equipment for data exchange. The main target of this thesis is to explore the human body as a signal propagation channel. For this purpose, the limb

joint effect of human body has been investigated, the characteristics of baseband digital signal transmission have been analyzed, and the suitable IBC system architecture has been developed.

The aims of this study are to

- Investigate the effect of body postures on the human body channel characteristics when data transmission is a baseband digital signal.
- Characterization of baseband digital signal propagation including pulse duty cycle and signal timeslot occupancy.
- Implement an IBC system for coupling signal current through human body and experimental evaluation of human body channel.

1.5. Outline of the Thesis

This thesis includes 5 parts in the following chapters.

- Chapter 2 highlights the background for this thesis. It introduces the most popular multiplexing types and modulation schemes of a digital communication system. Digital baseband IBC and IBC coupling methods are also presented. It also reviews the main papers discussing IBC transceivers.
- Chapter 3 presents the research methodology as well as experimental equipment. It details the IBC system testing safety requirements and measurement setups used in following chapters. It also reports empirical studies that explore signal propagation through the human body including limb joints. Those new empirical results demonstrate that the frequency

CHAPTER 1. INTRODUCTION

affects signal attenuation and pulse shape during IBC method through human arm.

- Chapter 4 presents preliminary channel attenuation characteristics implemented based on baseband digital signal transmission. The effects of duty cycle and timeslot occupancy are examined in this chapter.
- Chapter 5 demonstrates an IR type transmitter structure for carrier-free PPM scheme IBC application on FPGA implementation with galvanic coupling methods. The characteristics of the proposed IBC system such as path loss, noise, SNR, and BER are examined through the human body in our work.
- Chapter 6 proposes the remaining challenges and the future research work based on our measurement results.

Chapter 2

Background

This chapter aims to highlight the background of IBC communication system. Multiplexer and modulator are two major blocks of digital communication system diagram. The most popular multiplexing types and modulation schemes will be introduced for digital communication system at Section 2.1 of this chapter. In the following Section 2.2, the concept of digital baseband system and two basic IBC coupling methods are also presented. In the final part of Section 2.2, it also reviews the latest state of the art IBC transceiver designs and implements.

2.1 Digital communication systems

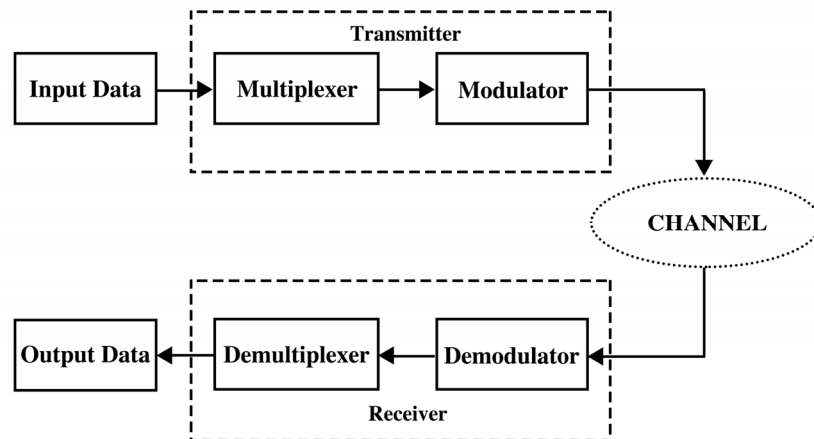


Fig. 2.1 Basic elements of a digital communication system

Generally, any communication system has three blocks which are transmitter, receiver and communication channel. Fig. 2.1 illustrates the diagram of a digital communication system including the basic elements. The transmitter side consists of modulator and Multiplexer. On the other side, the receiver part includes a demodulator and demultiplexer. The communication channel provides the connection between the transmitter and receiver. The signals always suffer distortion, attenuation and noise due to its propagation over the communication channel. The important parameters of the communication channel are signal to noise ratio (SNR), bandwidth, path loss and the noise. Shannon sampling theorem shows the relationship with SNR, bandwidth, noise and channel capacity.

2.1.1 Shannon sampling theorem

In communication systems, data rate usually refers to the information transmission in

CHAPTER 2. BACKGROUND

unit of bit per second while the bandwidth refers to the operation frequency in Hz. Channel capacity is the theoretical maximum data rate that is able to be transmitted through the channel with acceptable bit error probability, namely bit error rate (BER). It is the communication performance that can be calculated by the bandwidth and signal-to-noise ratio SNR of the given channel.

Additive white Gaussian noise (AWGN) is a basic noise model used in information theory to mimic the effect of many random processes that occur in nature. For an AWGN channel, Shannon-Hartley Theorem expresses the channel capacity C as

$$C = B \log(1 + SNR) \quad (2.1)$$

Where C is the channel capacity of communications, B is the bandwidth and SNR is the signal-to-noise ratio.

SNR can be further related to the bandwidth as

$$SNR = \frac{P_{sig}}{NB} \quad (2.2)$$

Where P_{sig} is the signal power and N is the noise power spectrum density.

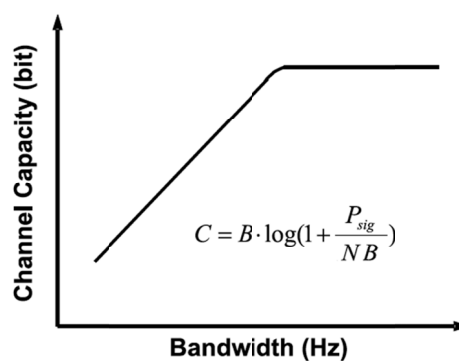


Fig. 2.2 Channel capacity against bandwidth for channels under AWGN

According to the Shannon theorem, data rate is theoretically limited by the channel capacity (see Fig.2.2). Increasing SNR could lead to high data rate, but it also cost high power consumption and interference with other wireless networks. Another option for achieving high data rate is to wisely choose modulation and multiple access techniques. Communication system design aims to ensure that the data rate is pushed as close as possible to the channel capacity limit.

2.1.2 Multiplexing

Multiplexing is a technique that places multiple signals into a same medium. In communication system, multiplexing means combining multiple signals to be sent over a shared transmission medium. The common multiplexing techniques include.

- Frequency Division Multiplexing (FDM): FDM achieves the combining of several signals into one medium by sending signals in several distinct frequency ranges over a single medium.
- Code Division Multiplexing (CDM): each signal is assigned a unique code sequence for modulation; all signals are allowed to be transmitted over the same channel simultaneously.
- Time Division Multiplexing (TDM): divides the available transmission time into timeslots, allocates a different timeslot to each signal and only one signal is allowed to occupy in each timeslot.

In digital communications, TDM advantage over FDM and CDM is that it provides bandwidth saving by dynamically allocating more time periods to the signals that need more of the bandwidth and low interference between the signals that are being

multiplexed in time.

In TDM system, timeslot is a short duration of time divided by the system for signal occupancy. The multiplexing operation provides an opportunity for each signal to occupy one or more timeslots. Time is segmented in to intervals called frames. Each frame could be further distributed into assignable signal timeslots.

2.1.3 Modulation scheme

The purpose of a communication system is to transfer information through communication channel from a source to a destination. We can see at Fig. 2.1, there are two blocks between source and communication channel. After Multiplexing, there should be a modulator following. Digital modulation is to represent the digital data in terms of electrical pulses transmitted over communication channels. The digital data transmission system should have acceptable complexity, high data rate and be energy efficient. An optimal modulation scheme should address the above factors.

There are several potential modulation scheme candidates for designing the IBC communication system. Based on amplitude, frequency and phase shifting, Amplitude-shift keying (ASK), frequency-shift keying (FSK), and phase-shift keying (PSK) are three of popular digital modulation schemes.

ASK is an amplitude modulation that distributes bit values to different amplitude levels. The strength of a signal is varied to represent binary 1 or 0 while both frequency and phase remain constant. Since noise affect the amplitude more than frequency and phase, ASK is vulnerable to noise interference. However, it has advantage of simplicity which means simple system architecture, low power

CHAPTER 2. BACKGROUND

consumption and low implementation cost.

FSK is a frequency modulation that assigns bit values to different frequency levels. The frequency of signal is varied to represent binary 1 or 0 with peak amplitude and phase remain constant during each bit interval. The detection of frequency variation over several intervals is easier than voltage with noise interference. Therefore, ASK is more noise sensitive compared to FSK, but FSK occupies double the spectrum width because of the requirement of two different frequencies for binary digital data representation.

PSK is another major digital modulation technique. This phase modulation assigns bit values to different phase angles. During each bit interval, instead of frequency (FSK) and amplitude (ASK) variation, the phase of signal is shifted between two or more values for digital data representation. Although PSK is less susceptible to errors than ASK, it has more complex signal circuitry.

In short, compromising with bandwidth and power requirement, ASK should be the most potential modulation scheme for IBC communication system. As the simplest form of ASK modulation, On-off keying (OOK) allows the transmitter to be idle during binary 0 transmissions thus achieving energy efficiency.

If we consider the multiple signals transmitted over the same communication channel, the multiplexer (see Fig. 2.1) in front of modulation could offer the method which for signal transmission sharing the same channel. It maximizes the utilization of the communication channel. If these signals are multiplexed in time, it is called TDM. Pulse position modulation (PPM) is modulation technique which placed multiple sources into a same channel using TDM. In PPM, the pulse is present for short

CHAPTER 2. BACKGROUND

durations at specific time intervals. The other interval times could be occupied by the pulses from other sources. Transmitting a very short pulse with no radio frequency modulation is known as impulse radio (IR) [21]. For short distance data communications, IR is a suitable choice for lower power consumption and higher data rates [22]. IR typically has a simple structure in which the information data symbols modulate the pulses with a pulse position modulation (PPM) scheme [23].

Both OOK and PPM schemes use timeslot for binary data representation. In an OOK modulation system, the transmitter generates a pulse in a timeslot to represent “1”, no pulse for a “0” bit. On the other hand, in a PPM system, a symbol with $L=2^N$ timeslots corresponds to a symbol interval of N bits in OOK. The pulse is only sent by transmitter in one of L timeslots. The symbol is determined by the position of the active timeslot during L timeslots. Taking $L=4$ PPM for an example, the symbol structures of OOK and 4-PPM is showed in Fig.2.3.

Source bits	OOK	4-PPM
00		
01		
10		
11		

Fig. 2.3 Symbol structures for OOK and 4-PPM

Since PPM is a time-based technique, it has lower possibility to false detection compared to OOK which is a shape-based modulation scheme. Due to similar amplitude pulses of PPM, the detection of channel noise is simpler than OOK. Hence more robust and power efficient transmitters are provided by PPM [24]. As only one timeslot is active during the data transmission, PPM decreases the average power requirement occupied a larger bandwidth. Compared with OOK modulation, PPM modulation has lower average power, higher peak power and high SNR [25]. This study could be helpful for modulation scheme selection in the IBC communication system design. The details of PPM modulation scheme will be demonstrated in chapter 5 as part as the IBC system design.

2.2 IBC transmission system

Signal transmission around the human body has long been the center research topic for biomedical engineering in both academic and industrial areas. There are various applications using both external (on-body) and internal (in-body) devices. In IBC system, signals produced by various medical devices are not always suitable for direct transmission over a body channel. This leads to IBC system design investigation.

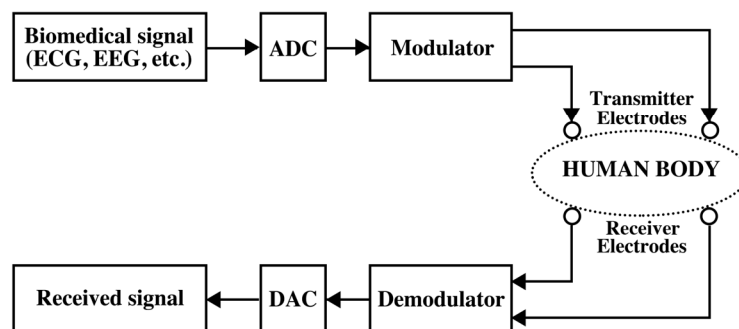


Fig. 2.4 Simplified block diagram of the IBC transceiver system

Normally, the transmitter part includes a modulator, an encoder and an analog-to-digital converter (ADC) (see Fig. 2.4). The receiver part consists of a demodulator, a decoder and a digital-to-analog converter (DAC). The communication channel is the transmission path the signals propagate through. In IBC system, the human body itself causes transmission signal loss and distortion.

2.2.1 Baseband communication system

Generally, the communication systems can be classified to two models depending on their data transmission frequency band. They are baseband and passband system which is depicted in fig. 2.5 as the block diagram. Baseband transmission propagates the signal without frequency shifting while passband transmission shifts the signal into a higher carrier frequency for transmission. The carrier is a waveform that is modulated with input data. The purpose of the carrier is to facilitate information transmission through space as an electromagnetic wave for high quality data propagation. For baseband digital communication system, the data is represented by

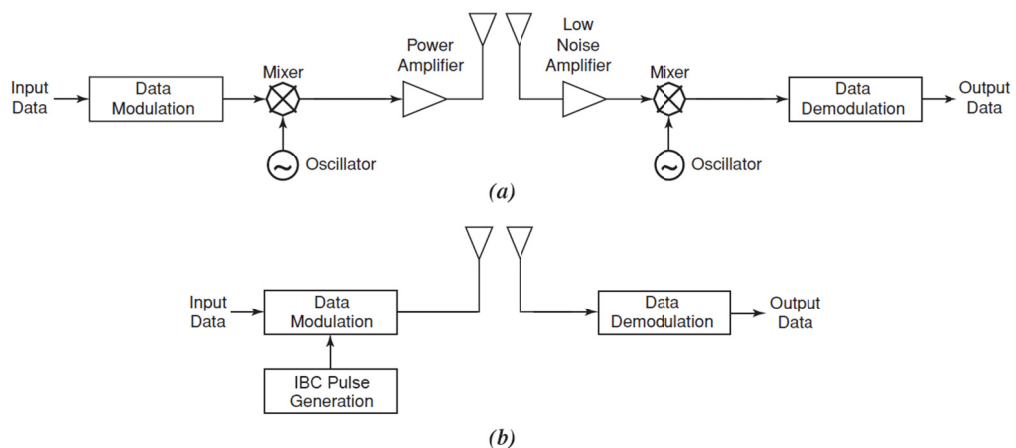


Fig. 2.5 Simplified block diagram of the (a) passband system and (b) baseband system

digital symbols that are assigned by pulse waveforms. This step is referred to as pulse modulation or baseband modulation.

As a short-range communication system, we propose that IBC be carrierless meaning that it is a baseband system. The IBC data is not modulated on a continuous waveform with a specific carrier frequency. IBC transceiver architecture is simpler because the carrierless transmission requires fewer RF components than carrier based transmission. In IBC transmitters, a power amplifier (PA) is not required because of low-powered pulses. There is also no need for mixers and local oscillators (LO) to add the carrier frequency in carrierless IBC system. In short, the analog front end of IBC system is less complicated making it low cost and easy design.

2.2.2 IBC coupling methods

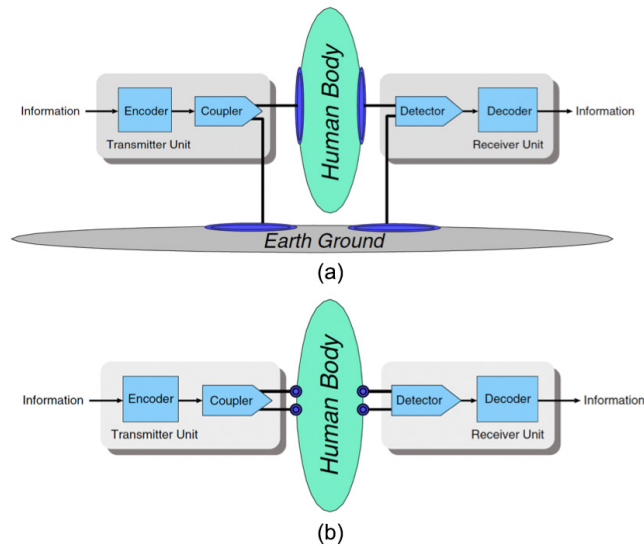


Fig. 2.6 Capacitive coupling and galvanic coupling for data transmission between transmitter and receiver units

CHAPTER 2. BACKGROUND

The principle of IBC is that small electric fields are intentionally introduced onto the human body in order to propagate a signal [19]. Methods for transmission in IBC can be divided to the two conceptually different approaches: capacitive coupling (electric field) type and galvanic coupling type (waveguide) (see Fig. 2.6) [26]. The induced electrical signal is controlled by an electrical potential or a current flow. In the capacitive coupling method, the transmitted electrical signal is capacitively coupled through the air or the ground. The method is also known as the near-field effect. The galvanic coupling method transfers the signal by injecting alternating current into the human body. In this method, the human body becomes a transmission line or waveguide.

Capacitive coupling: one signal path is established through the human body while the return path has to be connected by earth ground. Galvanic coupling: differential current is coupled into the human body by the pair of coupler electrodes and sensed by the pair of detector electrodes. Therefore, galvanic coupling doesn't require ground return paths.

Usually, in the capacitive coupling method, only the signal electrode of the transmitter and the receiver is attached to the human body while the ground electrode is floating. In galvanic coupling IBC, however, both transmitter and receiver electrodes are attached to the body and the electrical signal is applied differentially between the two electrodes of the transmitter. Governed by the dielectric properties of human body tissues, i.e. relative permittivity (ϵ) and electrical conductivity (σ), the major portion of the electric current in this method flows between the two transmitter electrodes while a small portion flows toward the two receiver electrodes. This small current results in a potential difference that is detected differentially by the receiver electrodes. The galvanic coupling method was less influenced by the environment compared to

CHAPTER 2. BACKGROUND

the capacitive coupling method. Since the capacitive coupling has a return path going through the parasitic earth ground, it becomes highly susceptible to external interference, such as power lines (50 Hz mains) and other nearby WBAN devices. The current propagation in galvanic coupling, however, takes place within the human tissue layers and the body tends to screen out external interfering signals.

The galvanic coupling method was investigated within a higher frequency range for achieving higher data rate. It has interest to investigate galvanic coupling method, since it is less susceptible to environmental effects (current predominantly flows through tissues) compared with capacitive coupling IBC. In this thesis, the experimental results is measured based on galvanic coupling method with the proposed IBC system.

2.2.3 Current IBC communication systems

The operation frequency of IBC system leads to propagation gain characteristics that affect the transmission wave shape. The distance of communication channel also influences the path loss that may affect SNR and channel capacity (see equation 2.1). Experimental results of IBC testing system could achieve deeper understanding of the human tissue acting as the transmission medium.

IBC has been employed for telemedicine science with the large improvement of wireless communication technology. The novelty of IBC is the use of the human body itself as the signal propagation medium. The detailed characteristic of human body is still under investigation. This section reviews IBC communication system by introducing and comparing different IBC transceivers design.

CHAPTER 2. BACKGROUND

- A. The initial near-field PAN transmission prototype was proposed by Zimmerman in 1995 [18]. The human body was used as transmission medium because of its better conductivity than air. OOK modulation was employed to achieve a simple structure and cost efficient design. In his work, he suggests capacitive coupling method used at WPAN, because the PAN equipment are located to feet (near the physical ground) to optimize received signal amplitude. Transmitter and receiver have separate isolated grounds. The carrier frequency range is set from 100 kHz to 500 kHz to achieve a data rate of 2.4 kbps. However, this data rate is unable to fulfill the requirement of sensors sending high data rate (EMG).

- B. Galvanic coupling approach is first present by Hachisuka, *et al.*, [27]. The different size or material of electrodes and the optimized carrier frequency range (10-30 MHz) were considered. The measurement also investigates the different arm positions as the different channel gain. For instance, the gain is higher when the arm held up or held horizontally, and it is lower when the arm held down. The frequency modulation (FM) (carrier frequency = 10.7 MHz) and FSK are used transmitting the analog and digital data through human body. The experiment results show that the signal is received correctly with 9.6 kbps data rate. Again, the proposed transceiver system suffered from low data rate.

- C. In the work [28], it is investigated the galvanic coupling approach which is suitable for on-body sensors in biomedical monitoring systems. The measurement results are analyzed for the signal transmission attenuation evaluation on human body channel. The study considered about the effect of human body joint, distance between transmitter and receiver and types of electrodes. The battery powered field programmable gate array (FPGA) transceiver was implemented in

CHAPTER 2. BACKGROUND

order to isolate the sensor unit from other power line. FSK and binary phase shift keying (BPSK) modulations are used for digital data transmission at different frequencies (10 kHz, 100 kHz, 500 kHz and 1 MHz). The BPSK data rate achieves 255 kbps with a 600 kHz carrier frequency. Unfortunately, the data rate of this proposed system is still not high enough to achieve some biomedical applications such as image transmission of medical implant communications.

- D. This paper proposed a dual mode IR system using PPM scheme for both in-body (3.4-4.8 GHz band) and on-body (20-60 MHz band) communication [29]. It formulated the path loss characteristics and BER performance. They employed oscilloscope and spectrum analyzer instead of receiver. However, neither data rate nor power consumption measurements were performed, because only transmitter side was developed. The receiver design is another important issue of IBC system.
- E. In this study, an IBC transceiver based on OOK modulation scheme is presented for WBAN [30]. The carrier frequency for OOK is optimized to 30 MHz. A FPGA board is implemented to achieve OOK modulation in the IBC transmission system. The not return to zero (NRZ) test code is transferred from forearm to finger through the human body with 2 Mbps. However, the NRZ data generated by FPGA board is only for testing. It is not only doubled the power consumption of transmitter but also not for the real world.
- F. In this work, an IR type transceiver based on OOK modulation scheme is developed for IBC application [19]. With the transmission spectrum (30 -50 MHz), the signal propagated through human body with low path loss. The signal's attention is around 50dB at the body surface distance of 50 cm. Its

CHAPTER 2. BACKGROUND

communication performance has been evaluated for achieving 1.2 Mbps data rate on-body transmission. Although the data rate of their system is acceptable for medical sensors (EMG), the path loss against channel distance on body surface should be mathematically modeled and compared with the theoretical and empirical data.

- G. In this paper, the authors focus on the evaluation for IR-UWB transmission with PPM scheme [31]. Instead of IBC, it's a RF transmission system. The performance of PPM scheme was evaluated for IR-UWB transmission system operated with low band (3.4-4.8 GHz). To this end, the authors developed an IR-UWB communication system with PPM scheme. Through the experimentally evaluation of the transmission performance of the proposed system, the authors theoretically analyze the bit error rate (BER) performance by using Gaussian approximation. The proposed system has achieved the BER as 10^{-2} at the path loss of 75 dB with the 2 Mbps data rate. However, they employed the attenuator instead of a living human body for measurement.

CHAPTER 2. BACKGROUND

A list of IBC system above is shown in TABLE 2.1.

TABLE 2.1 Summary and comparison of current IBC communication system

Author (year)	Coupling Method	Carrier Frequency	Modulation Technique	Date Rate
Zimmerman (1995)	Capacitive	330 kHz	OOK	2.4 kbps
Hachisuka (2003)	Galvanic	10.7 MHz	FSK	9.6kbps
Wegmueller (2005)	Galvanic	600kHz	BPSK	255kbps
Shi (2011)	Capacitive	20-60MHz 3.4-4.8GHz	PPM	Not Reported
Leng (2011)	Capacitive	30MHz	OOK	2Mbps
Shikada (2012)	Capacitive	30-50Mhz	OOK	1.2Mbps
Katsu (2013)	Capacitive	3.4-4.8GHz	PPM	2Mbps

2.3 Conclusion

This chapter provides a survey of research in IBC transmission method. We reviewed the multiplexing and modulation schemes of IBC, IBC coupling methods and current IBC transmission systems. The Reliability, power consumption, data rate and security are main considerations of wireless communication system design. Based on the

CHAPTER 2. BACKGROUND

human body channel limitations and body tissues characteristics in different frequency domain, direct data transmission through the human body lead to a large transmitted voltage or power. The analyzed measurement results should include bit error rate (BER), SNR and signal strength level with respect to propagation distance. The performance of the IBC transceiver in terms of path loss, noise, SNR, channel distance effect and BER should be evaluated based on the waveform distortion and human body channel measurement. Based on the above, in this thesis, we demonstrate an IR type transmitter structure for carrier-free PPM scheme IBC application on FPGA implementation with galvanic coupling methods.

Chapter 3

Limb Joints Effect

IBC is one of the recent physical layers of the IEEE 802.15.6 WBAN communication standard. It is employed for data transmission in low frequency bands (21 MHz as per standard, 0.3-120 MHz in literature), providing up to 10 Mbps data throughput. Due to the different human tissue layers with other parts of human body, the joints in IBC pathway affect the signal propagation. The joint effect analysis will be helpful for the evaluation of the signal propagation characteristics. Since the arm is commonly used as monitor points in medical applications, the influence of joint segments in the IBC channel is required for more research.

An effective way to increase data rate communication is to determine higher operation frequency bands. The electromagnetic interference is one of the most significant factors for transmission frequency range determination of IBC communication system.

CHAPTER 3. LIMB JOINTS EFFECT

The frequencies below 0.1 MHz is sensitive to all types of electromagnetic interference. According to Gabriel *et al.*, [33], the conductivity of human body issue is almost constant during 0.1–200 MHz frequency range. Therefore, electrical properties of human body tissues could act constant for this frequency range measurement. The maximum IBC data rate is reported as 1312.5 kbps in the 21 MHz frequency band by IEEE WBAN standard. Although, this data rate is suitable for medical data transmission, e.g. capsule endoscope and glucose monitoring, some healthcare applications such as medical imaging require higher data rates above 10 Mbps [34]. The operation frequency band therefore needs to be enhanced in order to increase the data rate of IBC communication system.

This chapter reports empirical studies which explore signal propagation through the human body including limb joints within the 0.3-200 MHz frequency range. Results show that minimum signal attenuation points occur at 50 MHz and 150 MHz within the range of investigation. The presence of the joint segments along the signal propagation path causes on average 2.0 dB loss (at 50 MHz and 150 MHz), 6.0 dB loss (<1 MHz) and less than 3.0 dB (>150 MHz) compared to limb segments.

3.1 Methodology

Recent IBC research has investigated the signal propagation through the body channel. With the *in-vivo* measurement system setup, the galvanic coupling IBC will be evaluated by investigations of signal variations on different human body parts. The proposed methodology will also be employed for the investigations of human body channel characteristics in chapter 4 and 5.

3.1.1 The preparation for measurement

Generally, each communication system has three fundamental blocks which are transmitter, receiver and propagation channel. Since human body is the communication medium of IBC system, safety and medical requirement should be fulfilled for live human body experiments. In this study, ethics approval was obtained from *Victoria University Human Research Ethics Committee* (VUHREC) to investigate empirical measurements on the human body.

3.1.2 Measurement system design

The empirical measurements were analyzed to demonstrate the signal transmission performance through human body tissue. The IBC system is composed of connecting cables, balun transformers, the surface electrodes, human body tissue as communication channel and electronic devices that function of as transmitter and receiver.

During the measurement, two pairs of hypoallergenic surface electrodes were equipped at transmitter and receiver sides. Those electrodes are used as communication interface between electronic equipment and body skin tissue. In our measurement, the single commercial silver/silver chloride (Ag/AgCl) electrode (Noraxon Inc., Scottsdale, AZ, USA) was employed. These electrodes are popular in monitoring systems such as EMG systems. Additionally, employing the self-adhesiveness of Noraxon electrodes keeps them stable during human subject movement.

CHAPTER 3. LIMB JOINTS EFFECT

The differential amplifiers or balun (balance-unbalanced) transformers were employed to eliminate the undesired common mode signals from power line interference. They prevent the signal return path from being shorted to the common voltage. The two baluns (FTB-1-1+, mini-Circuits Inc., Brooklyn, NY, USA) are used in measurements. Fig. 3.1 shows the schematic diagram of the coaxial balun transformers which cover the wide frequency band of 0.2-500 MHz. Moreover, since the presence of baluns can affect the channel response, the measured transmission coefficient of the balun is demonstrated in Fig. 3.2.

The pair of baluns decouples the ports from each other. They also transform a single-ended (unbalanced) signal into a differential (balanced) signal that is required for the galvanic coupling IBC. The coaxial balun transformers cover the wide frequency band of 0.2-500 MHz. These balun transformers are placed between electrical equipment ports and connecting cables. It should be noted that the IBC measurement without baluns has 3 to 5.5 dB less loss compared to the setup with baluns, below 80 MHz. This could be explained by the presence of common ground in the measurement setup without baluns. The baluns on both transmitter and receiver sides isolate the interference from common ground during the signal transmission. However, it also introduced the signal attenuation (loss) because of its own internal electrical characteristics.

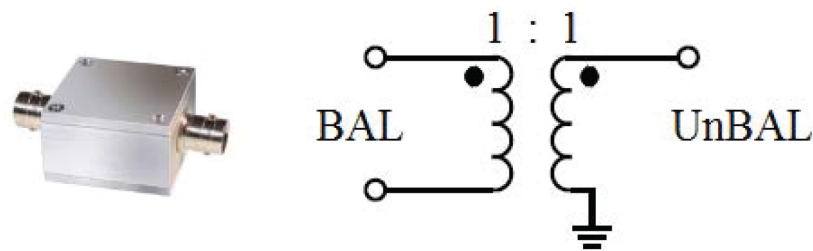


Fig. 3.1 The schematic diagram of the employed balun in the measurement setup

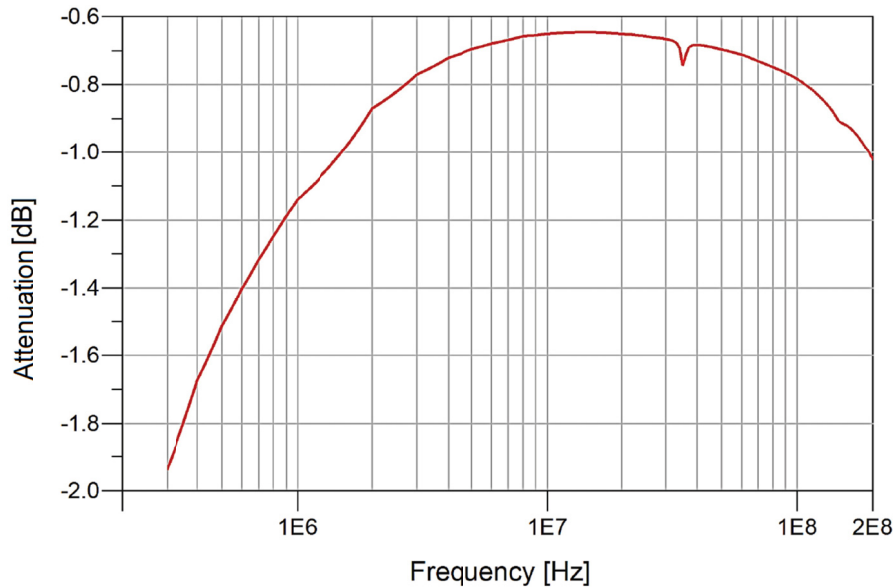


Fig. 3.2 The balun loss at desired frequency range of this study

3.1.3 Test protocol

4 healthy subjects volunteered to participate in this study. All subjects signed the consent forms mandated by the VUHERC. According to ICNIRP (“International Commission on Non-Ionizing Radiation Protection”, 1998) [35] exposure guidelines, the maximum transmission power for an average weight of 65 kg would be 37 dBm (= 5 W). The signal generator was set to a low input value of 1.0 V for safety reasons. The impedance of both transmitter output and receiver input was 50 Ω . During measurements, both transmitter and receiver electrodes were connected to the body in differential input mode and the inter-electrode distance was found to be 3.8 cm. The subjects were told to stand and hold their left arm horizontally (parallel with earth ground). The measurements for each position were repeated three times over several days and the average was reported.

3.2 Experiment setup

Propagation of signals through the human body in IBC is largely governed by human tissue electrical properties. The two major properties are relative permittivity (ϵ_r) and electrical conductivity (σ). The most comprehensive overview on human body electrical properties is presented by Gabriel *et al.* in 1996 [33]. Experiments were performed on human and animal tissue within the frequency range of 10 Hz to 20 GHz. During the experiments the temperature was fixed (37°C) and it was assumed that tissue layers were homogenous. Fig. 3.3 shows the dispersion of relative permittivity and specific conductivity of human body tissue. The electrical properties of human tissue are a key element (feature) for designing an energy efficient, low noise, and cost effective IBC transceiver system achieved through the modeling of the human body transmission channel characteristics.

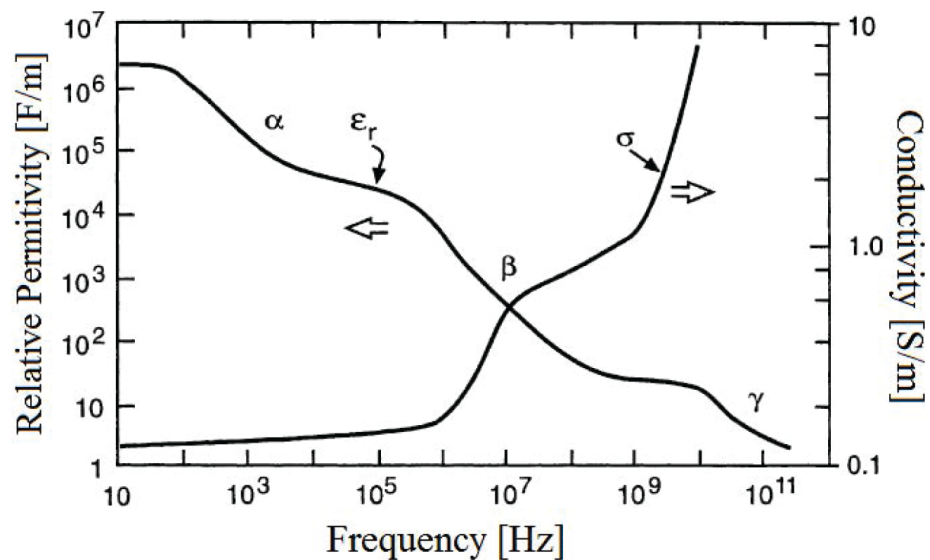


Fig. 3.3 Variation of human tissues electrical properties, relative permittivity and conductivity, against frequency [33]

CHAPTER 3. LIMB JOINTS EFFECT

The signal communication path in IBC is not similar to regular transmission paths in other communication technologies. The received signal by the IBC receiver electrodes needs to be evaluated in terms of different composition of the body segments. Research studies acknowledge that the human body response to the applied electrical stimulus is mainly influenced by first, the dielectric properties (ϵ , σ) of biological tissues and cell suspensions and second, the thickness of body tissues (d). Based on the research of Gabriel *et al.*, the dielectric properties of tissues highly contribute to determining the level of current penetration in deeper layers of human body tissue. The second factor which influences the signal behavior in biological tissues (d) is the thickness of body tissue layers. For instance, the bone layer thickness in the joint segments is more than other parts of the body such as the forearm. Based on (3.1) and (3.2), the impedance of various body tissue layers, which are modeled as RC -parallel networks, is calculated as following:

$$C = \epsilon \frac{A}{d} \quad , \quad G = \sigma \frac{A}{d} \quad (3.1)$$

$$Y = (\sigma + j\omega\epsilon) \frac{A}{d} \quad , \quad Z = \frac{1}{Y} \quad (3.2)$$

where C and G are the capacitance and electrical resistivity, A is the cross section area, and Z is the impedance of the body tissue layers. Therefore, to evaluate the IBC received signal by receiver electrodes, different composition of the body segments should be taken into account.

In this work, the pulse wave shape was transmitted through the body in different frequencies while the amplitude was constant. The attenuation or channel loss was calculated using (3.3):

$$\text{Attenuation} = 20\log_{10} (V_{\text{out}}/V_{\text{in}}) \quad (3.3)$$

CHAPTER 3. LIMB JOINTS EFFECT

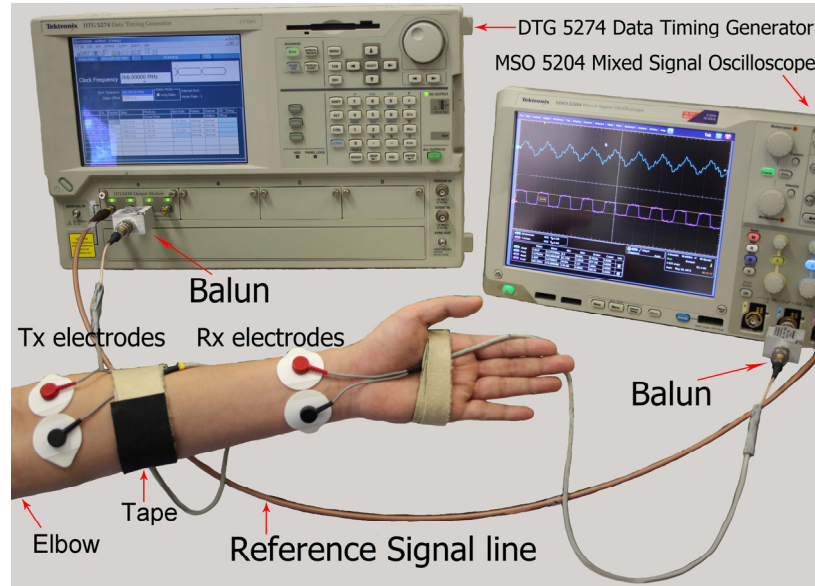


Fig. 3.4 The measurement setup of the IBC technique

where V_{in} and V_{out} depicts the amplitude of the transmitted and the received signal respectively.

Fig. 3.4 shows the measurement setup for the IBC experiments. A signal generator (DTG 5274, Tektronix, Inc.), a 50Ω balance-unbalanced (balun) transformer (FTB-1-1+, Minicircuit, Inc.), and a pair of commercial self-adhesive Ag/AgCl single electrodes (Noraxon, Inc.) were used in the transmitter side. A similar balun (0.2-500 MHz range) and electrodes including an oscilloscope (MSO 5204 Mixed Signal Oscilloscope, Tektronix, Inc.) were employed in the receiver side.

The data generator provided 1.0 V amplitude pulse with 50% duty cycle at different frequencies between 0.3-200 MHz. For instance, Fig. 3.5 shows a 50 MHz pulse wave measured by the oscilloscope. It was generated by the signal generator for transmission into the IBC channel. A pair of transmitter electrodes was employed as

CHAPTER 3. LIMB JOINTS EFFECT

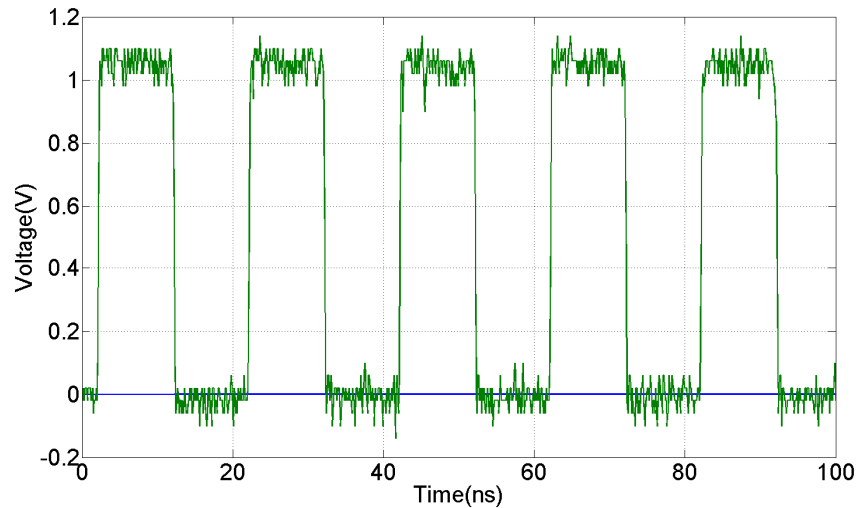


Fig. 3.5 Source transmitter waveform (50 MHz) measured by oscilloscope using IBC method

an interface to measure pulse waves at the body arm. Two EMG snap leads, with 115 cm length, were used as connecting cables at transmitter and receiver sides. Meanwhile, a coaxial cable was connected directly from the pulse generator to the oscilloscope as a reference.

In the first experiment, receiver electrodes were attached to the subject's left forearm and the transmitter electrodes were positioned on the upper left arm to measure the influence of the joint-segment. The distance between transmitter and receiver electrodes was 20 cm, while the elbow joint was located in the middle (10 cm from transmitter and receiver respectively). In the next experiment, the electrodes of both transmitter and receiver were attached to subject's left forearm 20 cm apart, and the receiver electrodes were close to the wrist, to simulate the no joint condition on a limb segment of similar length. The subjects were told to stand and hold their left arm horizontally (parallel with earth ground) while the measured arm distance from earth was 128 and 152 cm for

CHAPTER 3. LIMB JOINTS EFFECT

female and male subject, respectively. At each position, the received signal was measured by the oscilloscope for pulse waves with different frequencies in 0.3-200 MHz band.

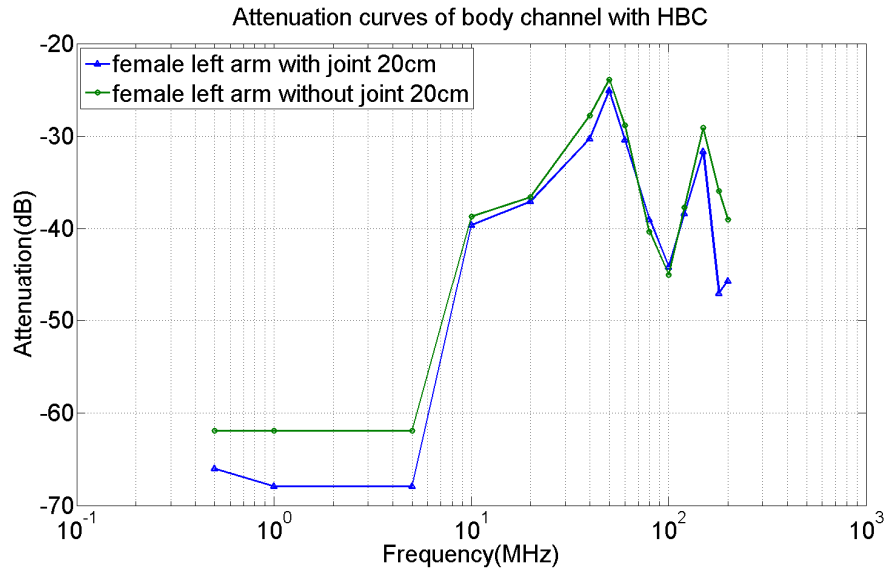
3.3 Measurement Results

The signal attenuation of the communication channel in this study was calculated by the received signal amplitude (see equation (3.1)). TABLE 3.1 shows the calculated attenuation for the male test subject for different frequency points. The yielded signal attenuation was then plotted against the frequency factor for both joint and no joint positions.

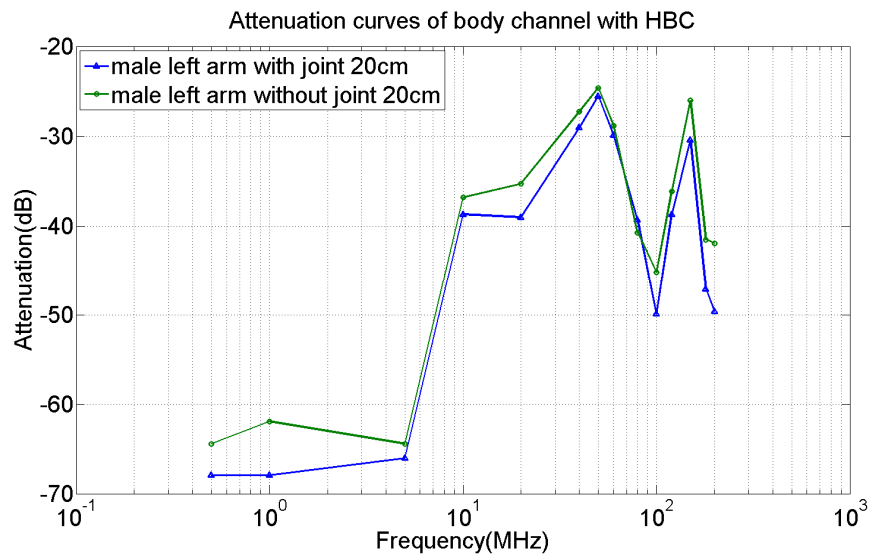
TABLE 3.1 The signal characteristics of male subject body during IBC

Frequency [MHz]	Received signal amplitude [mV] joint/no joint	Attenuation [dB] joint/no joint
0.5	0.4 /0.6	68.0 /64.4
1.0	0.4 /0.8	68.0 /61.9
10	11.6 /14.4	38.7 /36.8
20	11.2 /17.2	39.0 /35.3
40	35.2 /43.2	29.1 /27.3
50	52.8 /58.8	25.5 /24.6
60	32.0 /36.2	29.9 /28.8
80	10.8 /9.20	39.3 /40.7
100	3.20 /5.50	49.9 /45.2
150	30.0 /50.0	30.5 /26.0
200	3.30 /8.00	49.6 /41.9

CHAPTER 3. LIMB JOINTS EFFECT



(a)



(b)

Fig. 3.6 The signal attenuation of the arm for 0.3-200 MHz

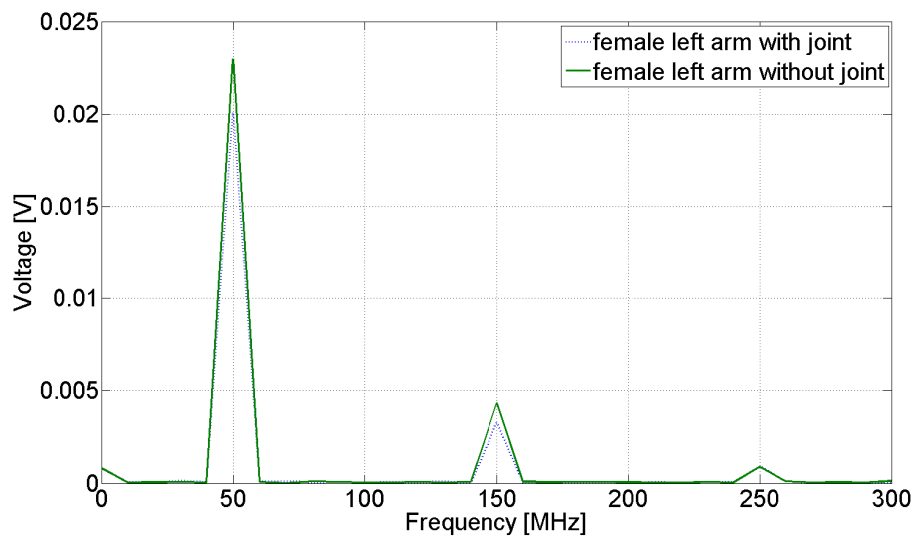
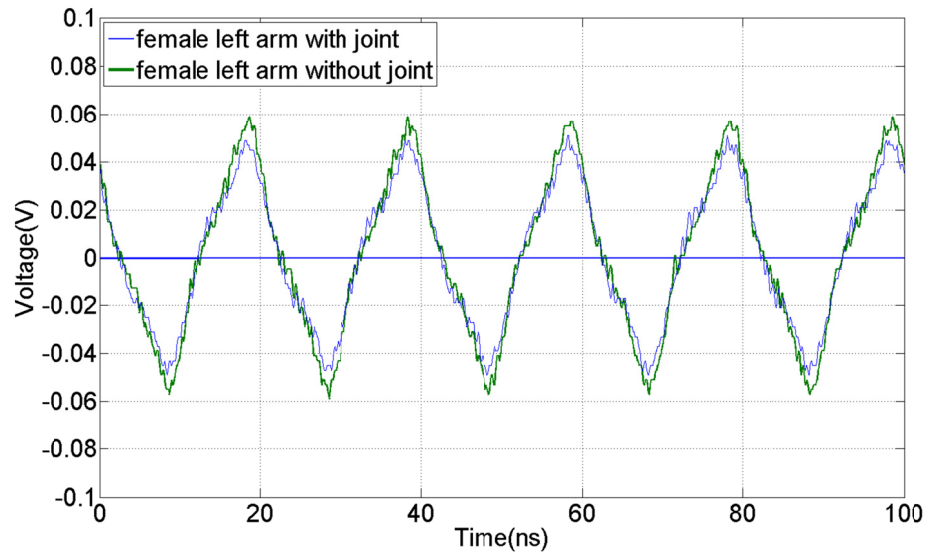
CHAPTER 3. LIMB JOINTS EFFECT

Fig. 3.6 (a) and (b) show the attenuation characteristics for both female and male subjects respectively. In Figure 3 (a), the channel attenuation for joint and no joint transmission was, respectively, 65 and 61 dB below 5 MHz. The attenuation decreases almost linearly to 25 dB prior to 50 MHz and increases to 45 dB at 100 MHz. It then decreases to 31 dB and 29 dB (for joint and no joint positions respectively) for another minimum at 150MHz.

Fig. 3.6 (b) shows the variation of the attenuation for the male subject's arm, with and without joint. The variation shows a similar pattern to the female subject in the desired frequency range. Based on the empirical results, the lowest attenuation were found to be also at 50 and 150 MHz, 25.5 dB and 30.5 dB (with the elbow joint), respectively. The absence of the joint showed only an improvement of 2 dB in attenuation in these two frequencies. Following a gradual decrease to minimum attenuation points, both curves fall to around 47 dB at 100 MHz. Beyond 150 MHz, the attenuation increased sharply to 50 dB (in presence of elbow joint).

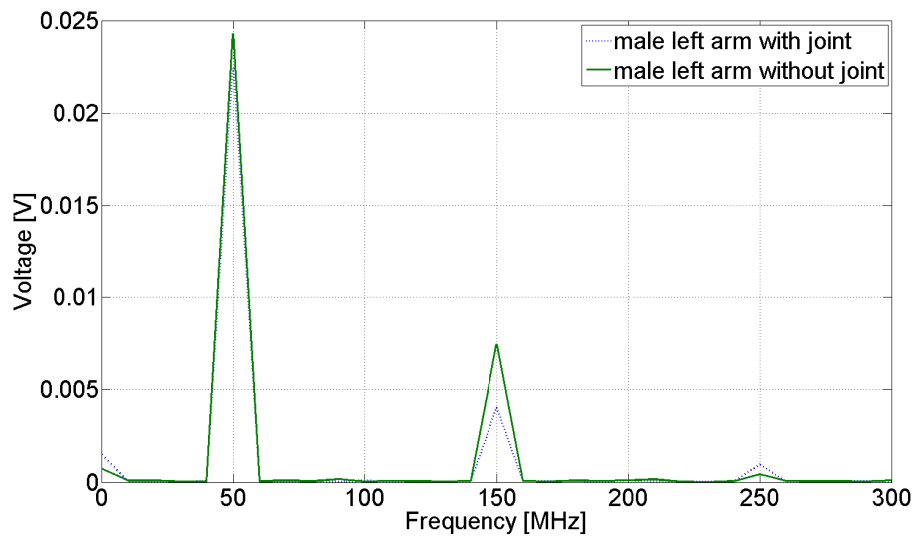
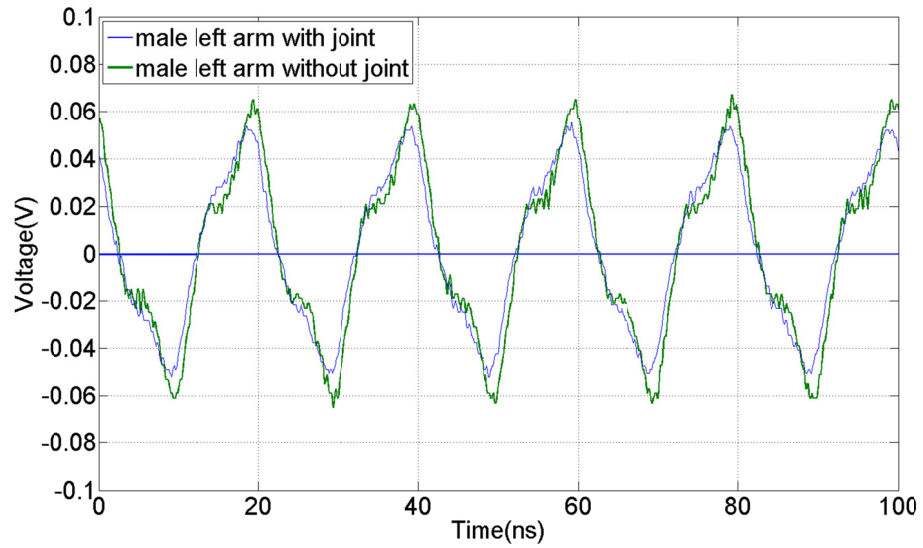
Based on Fig. 3.6, the minimum attenuation was observed at 50 MHz frequency. The received signal and fast Fourier transform (FFT) for both test subjects is shown in Fig. 3.7 (a) and (b). The results from both test subjects show that the received signal has lower amplitude when a joint is present. For example, the results from female subject's forearm (joint) show that the strength of transmitted signal decreased from 1 V to 118 mV (peak to peak) at 50 MHz frequency. In the same condition, the signal amplitude attenuates to 132 mV for the male subject. In addition, the output voltage difference between joint and no joint positions was less than 12 mV in peak points. The received signals are still periodic but do not appear to be square as per the transmitted signals (Fig. 3.5).

CHAPTER 3. LIMB JOINTS EFFECT



(a)

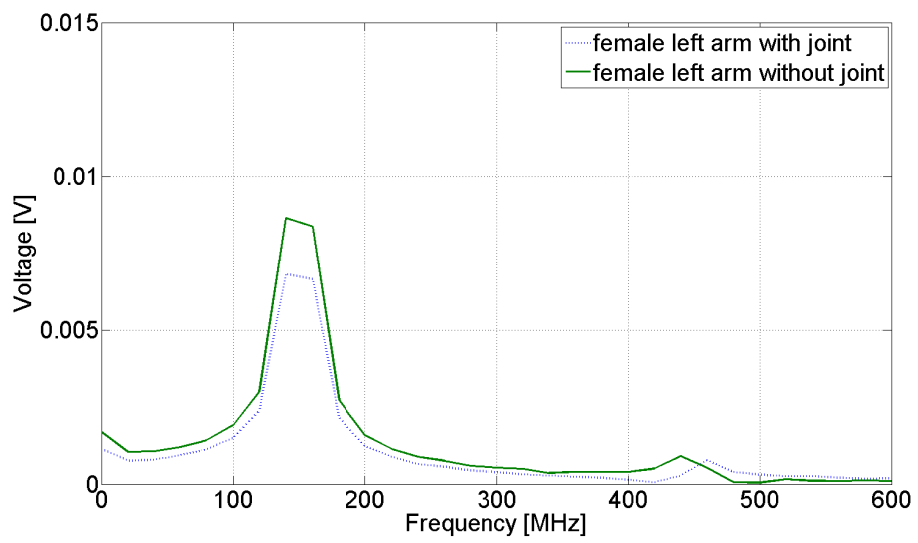
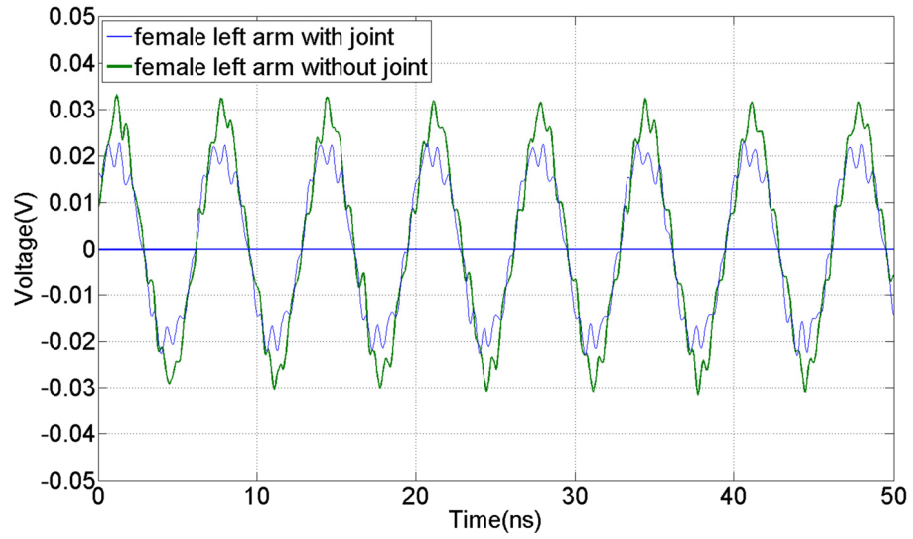
CHAPTER 3. LIMB JOINTS EFFECT



(b)

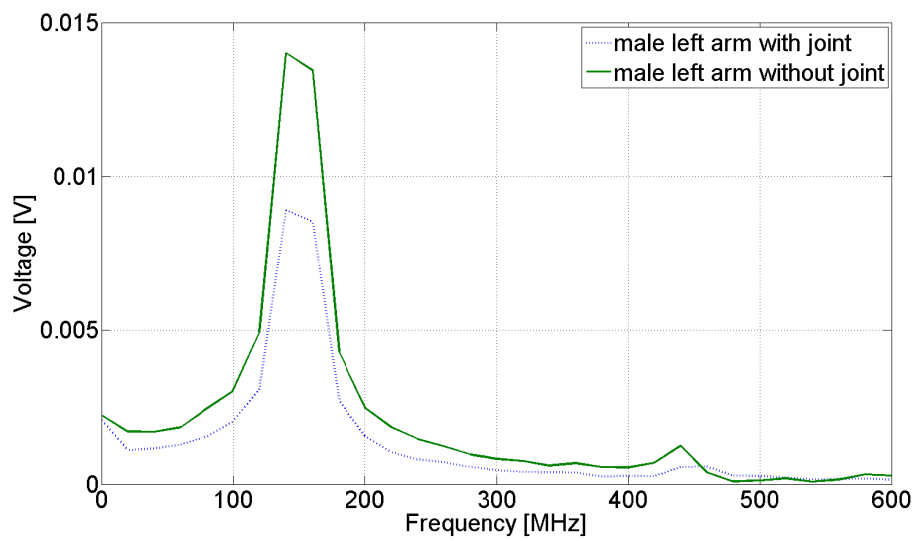
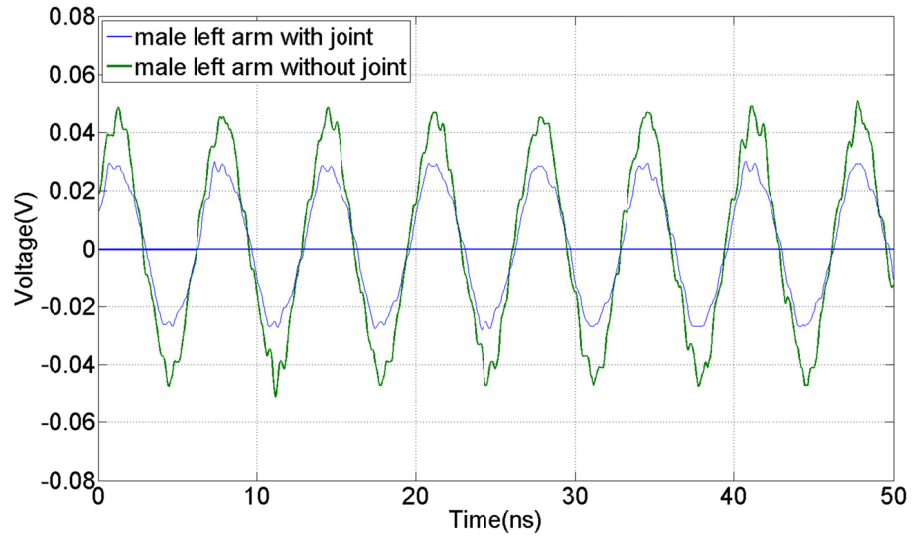
Fig. 3.7 IBC received signal and fast Fourier transform (FFT) in 50 MHz (a) female (b) male test subject

CHAPTER 3. LIMB JOINTS EFFECT



(a)

CHAPTER 3. LIMB JOINTS EFFECT



(b)

Fig. 3.8 Received signal and fast Fourier transform (FFT) in 150 MHz (a) female (b) male test subject

Fig. 3.6 indicates that the body channel loss is also low in frequency point of 150 MHz compared to other frequency points. The results of IBC system output and FFT are shown in Fig. 3.8 for both female and male subjects at 150 MHz. It is observed that the output voltage of received signal for female and male subject forearm is 66 and 102 mV, respectively. Meanwhile the received signal from body communication path without joint (body forearm) shows 15 mV higher voltage compared to the communication path with the elbow joint.

3.4 Discussion

Although IBC has been investigated by several researchers so far, there are still some major challenges to be addressed. The transmission characteristics of the human body is the key feature for designing a high data rate, energy and cost efficient IBC transceiver. Therefore, understanding the signal path loss and signal propagation through the body for both coupling techniques is of significant importance. Despite the existence of different human body communication approaches, they do not yet fully describe or predict empirical measurement results to determine the optimal frequency ranges. Another important factor that has received little attention is the presence of joint segments between the communication channel paths [36].

The variation of attenuation, observed in Fig. 3.7, is due to the different tissue layers and differing dielectric properties of the body tissue. The signal flowing in muscle is encounters less impedance than signals in other tissue layers. This could be attributed to the high salinity as well as the high water content of muscle (a good conductivity 0.678 S/m at 50 MHz with minimum attenuation) [33]. The attenuation curves (Fig. 3.6) could be divided into four different regions based on the frequency range: 0.3-50 MHz, 50-100 MHz, 100-150 MHz, and 150-200 MHz frequency bands.

CHAPTER 3. LIMB JOINTS EFFECT

It was observed that within the first frequency region the channel loss decreased when the frequency increases up to 50 MHz. This could be explained by the propagation of the signal through the body layers beginning from skin to fat and to muscle at the end (galvanic coupling). Above 50 MHz, the signal attenuation decreases (up to 100 MHz) potentially due to a major portion being coupled through the air (capacitive coupling). As frequency increases to 150 MHz, attenuation decreases potentially due to the decrease in the capacitive impedance of air. In 150-200 MHz frequency bands, the signal attenuation increases exponentially because energy is lost through electromagnetic radiation (the body acts as an antenna with skin effects). Future modeling work will be required to determine the primary coupling methods in these frequency ranges.

The effect of joint segments on signal attenuation in IBC appears to be more dominant in the low frequency range i.e. <1 MHz as the signal is predominantly coupled through the body tissues. Fig. 3.7 indicates that the presence of a joint between transmitter and receiver increases the signal attenuation between two limbs. The maximum attenuation difference between joint and no joint position was approximately 6.02 dB when transmission frequency was 1 MHz for both test subjects. For frequencies above 5 MHz, the attenuation differences between joint and no joint position was on average 1 dB and the difference decreased as frequency increased. The variation of attenuation could be explained by the unique composition of the joint segments where two or more bones meet together and muscle takes up a small portion. For instance, the linkage of the upper arm bone (humerus) with forearm bones (ulna and radius), through the elbow joint, creates larger impedance in the signal flowing path. Therefore, the signal has higher attenuation if a joint is present in the signal propagation path, more so at lower frequencies (<1 MHz).

CHAPTER 3. LIMB JOINTS EFFECT

Finally, the received signal of the IBC technique at 50 MHz and 150 MHz, as points with lowest attenuation, are shown in Fig. 3.7 and 3.8. It is worth noticing that the received signals are differentially received because balun transformers were used in the measurement setup, hence peak to peak transmitted signal is 0 to 1V and received signal is approximately -60 to 60 mV. At 50 MHz, the oscilloscope receives the signal amplitude of 51 and 59 mV for both joint and no joint position for the female subject. Although the presence of joint causes lower signal amplitude, the received signals have the same phase for both joint and no joint conditions, suggesting minimal phase shift effects. In summary, it appears possible to employ a higher frequency band (centered at 150 MHz) for IBC communications to construct a transceiver that will be less affected by movement i.e. limb joint effects. The results is in agreement with previous work [37] using a portable battery powered vector network analyzer (miniVNA Pro) instead of the signal generator and oscilloscope. The frequency band of IBC transceiver should be designed considering the human joint effect.

3.5 Conclusion

Decreasing the cost of the equipment, increasing the data rate, and finally fulfilling the requirements of the new WBAN standard remain significant challenges. We examined the 0.3-200 MHz frequency range for the IBC method to determine signal propagation characteristics at various frequency points. Based on the empirical measurements, it was found that body transmission channel loss was minimum at 50 MHz and 150 MHz. It was also found that the presence of a joint increased the attenuation less than 2 dB for these frequency points. Therefore, 50 MHz and 150 MHz should be the best frequencies for IBC transceiver implementation due to the lowest propagation loss comparing with other frequency ranges.

Chapter 4

Effect of user occupancy with baseband PPM

In this Chapter, we present preliminary channel attenuation characteristics of a TDM scheme implemented based on baseband digital signal transmission. A digital block implemented on a FPGA board as well as a digital Pulse Generator are employed as the IBC transmitters. The timeslot occupancy is simulated by adjusting the duty cycle of a square wave of varying frequencies. The measurements using FPGA indicate the signal attenuation of 32.76 and 27.82 dB at frequency of 10 and 25 MHz, respectively, for digital signals with 50% duty cycle. In addition, the attenuation of signal with 20% and 50% duty cycle at 50 MHz are 32.76 and 30.63 dB when Pulse Generator is used

CHAPTER 4. EFFECT OF USER OCCUPANCY WITH BASEBAND PPM

as the IBC transmitter. The variation of duty cycle in pulses was then used to simulate a time division multiplexed transmission scheme. It was observed that the attenuation decreases around 4.0 dB when data pulses are increasingly present from 1 to 5 timeslots. Therefore, digital baseband signals deployed in a time division multiplexed mode with higher timeslot occupancy leads to lower attenuation for IBC transmissions.

4.1 Experiment setup

Since the higher communication frequency range leads to higher data rate [20], the higher operation frequency band of 5.0-66.7 MHz, compared to the galvanic coupling IBC, is examined in this work. In this configuration, both electrodes are applied to the body and the signal is applied differentially. This is reminiscent of low frequency galvanic coupling IBC, but with an extension to the frequency ranges above 2.0 MHz (leading to capacitive coupling).

In this work, the digital baseband signals with different duty cycle and pulse timeslot occupancy were transmitted through the human arm using IBC technique. In order to generate the mentioned signals, two types of measurement equipment were established. In first measurements, a digital Pulse Generator as data transmitter in employed. In the second method, the baseband digital transmitter block was implemented on FPGA.

In both measurement setups, a digital square wave was transmitted through the body forearm with different frequencies and constant amplitude. The received signal amplitude is used to calculate the signal attenuation or path loss. Signal attenuation is the frequency response of the body channel to digital input signal. The signal attenuation has been computed as same as equation 3.3 (chapter 3). In both

CHAPTER 4. EFFECT OF USER OCCUPANCY WITH BASEBAND PPM

measurement types, similar instruments such as cables and oscilloscope were employed.

In this study, two kinds of transmitters were used to generate the digital baseband signal: a) Data Timing Generator (DTG 5274, Tektronix, Inc.) and b) digital transmitter implemented on FPGA board with clock frequency equal to 100 MHz (Xilinx Virtex5, Genesys, Inc.). The former was powered by mains supply while the latter was battery powered. Using VHDL program, we divided the clock of FPGA board into different frequencies and removed pulses in certain positions to emulate user occupancy in a timeslot. A $50\ \Omega$ balance-unbalanced (balun) transformer from Mini-circuit Inc. (0.2-500 MHz range) were used to remove the main power effects in the first structure. Neoprene straps (with Velcro) were used to fasten the cables to forearm to minimize movement artefacts. In both measurement setups, an oscilloscope (MSO 5204 Mixed Signal Oscilloscope, Tektronix, Inc.) was employed to detect the received signal. A pair of commercial self-adhesive Ag/AgCl single electrodes (Noraxon, Inc.) was used to provide impedance matching in the both measurement setups (see Fig. 4.1 and 4.2).

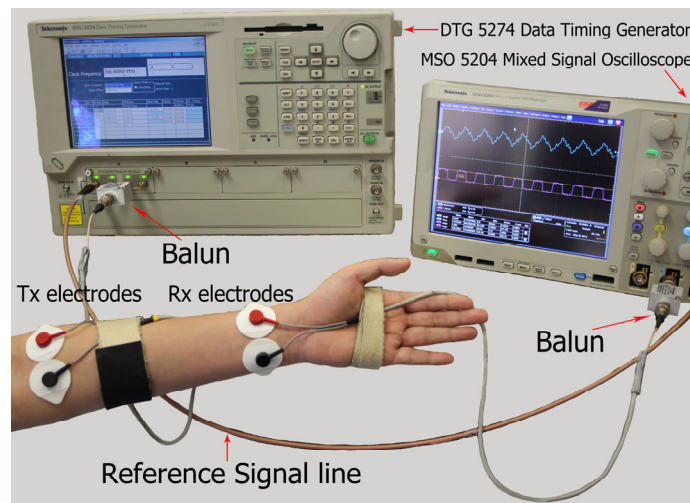


Fig. 4.1 The measurement setup using Pulse Generator and Oscilloscope (method a)

CHAPTER 4. EFFECT OF USER OCCUPANCY WITH BASEBAND PPM

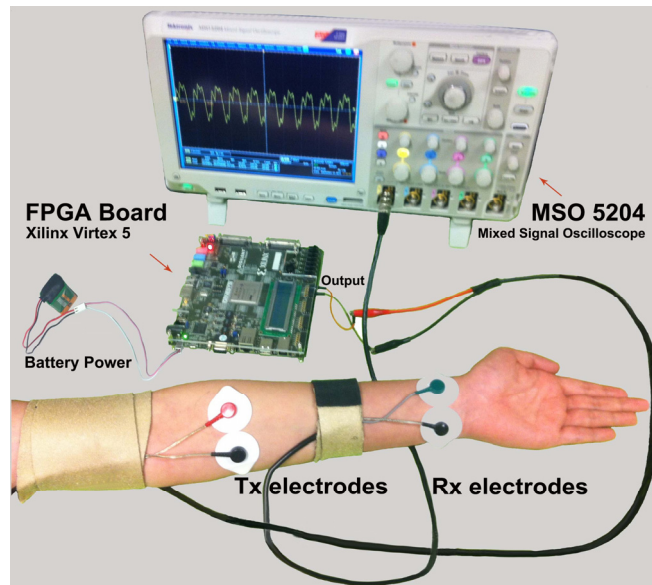


Fig. 4.2 The measurement setup of FPGA board and oscilloscope (method b)

In this study, two healthy volunteers (1 male and 1 female) participated in the experiments. The male subject was 30 years old, 182 cm height and 75 kg weight and the female subject was 27 years old, 162 cm height and 57 kg weight. The output amplitude of Pulse Generator and FPGA board were selected 1.0 V and 0.7 V, respectively, at the frequency range of 5.0-66.7 MHz which were considered safe for the human body [35]. During measurements, both transmitter and receiver electrodes were connected to the body in differential input mode.

In all experiments, the transmitter and receiver electrodes were attached on the subject's left forearm. The distance between transmitter and receiver electrodes was 20 cm. The receiver electrodes were close to the wrist and the transmitter electrodes were near the elbow joint (forearm). During both experimental conditions inter-electrode distance, i.e. distance between two electrodes of the same pair, was set to 3.8 cm. The

CHAPTER 4. EFFECT OF USER OCCUPANCY WITH BASEBAND PPM

subjects were asked to stand and hold their left arm horizontally (parallel with earth ground) while the arm distance from earth was 128 and 152 cm for female and male subject, respectively. At each experiment setup, the received signal was measured by the oscilloscope for pulse waves with different frequencies.

4.2 Results and discussion

4.2.1 Pulse Duty Cycle

Fig. 4.3 demonstrates the attenuation characteristics in the frequency range (10.0-60.0 MHz) for four different duty cycles of 20%, 25%, 33%, and 50% using the first measurement setup (see Fig. 1). The signals were propagated through the body by means of the Data Generator. The curves in Fig. 3 show that the signal with lower duty cycle suffer higher attenuation. The duty cycle could be used to simulate user occupancy in a TDM PPM scheme. For example, the half and one third of available

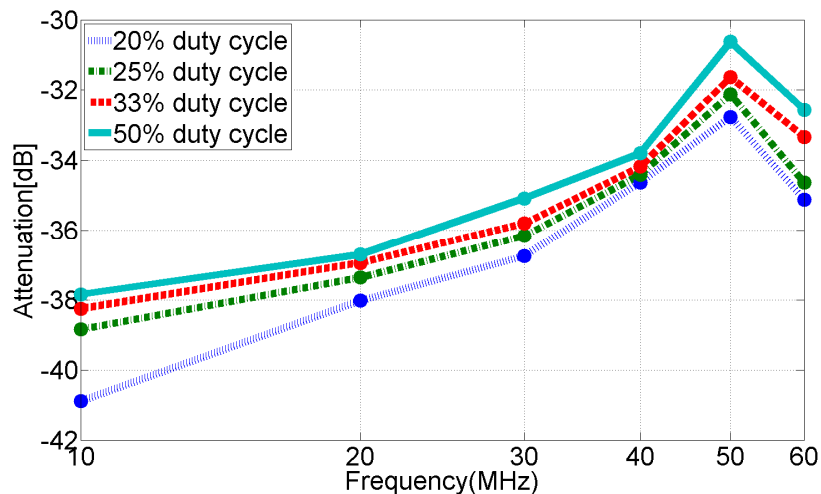


Fig. 4.3 The signal attenuation of the body channel for input signal with 20%-50% duty cycle when Data Generator was used as transmitter

CHAPTER 4. EFFECT OF USER OCCUPANCY WITH BASEBAND PPM

TABLE 4.1 The propagated signal characteristics at 50 MHz using pulse generator

Duty cycle (%)	Received signal amplitude [mV]	Attenuation [dB]
20	23.01	32.76
25	24.78	32.12
33	26.20	31.63
50	29.41	30.63

intervals are occupied by users if the signal duty cycle are 50% and 33%, respectively. This leads to low power spectrum density when the duty cycle of signal is low compared to signals with higher duty cycles. For instance, TABLE 4.1 shows the calculated signal attenuation at 50 MHz during different duty cycles of input signal.

Fig. 4.4 indicates the attenuation characteristics when our digital transmitter was implemented on a FPGA board in the frequency range 10.0-66.7 MHz with different duty cycles (20-50%). The curves show a similar behavior as Fig. 3, i.e. decreasing in attenuation values in the desired frequency range. It should be noted that, the inconsistency of frequency ranges in Fig. 4.4 was due to the programming limitation for different duty cycle curves. The FPGA measurement setup indicates higher attenuation compared to Data Generator measurements. This difference could be due to the presence of baluns. Therefore, the insertion loss of baluns (2.1 dB for each balun [38]) needs to be subtracted from attenuation of first measurement setup. As shown in both Fig. 4.3 and 4.4, all attenuation curves decreases linearly at frequencies less than 50 MHz. This could be explained in terms of the signal propagated through body tissue layers from skin to fat and then to muscle which has lower impedance. Therefore, lower body channel attenuation is obtained during higher frequency transmissions as well as higher duty cycles.

CHAPTER 4. EFFECT OF USER OCCUPANCY WITH BASEBAND PPM

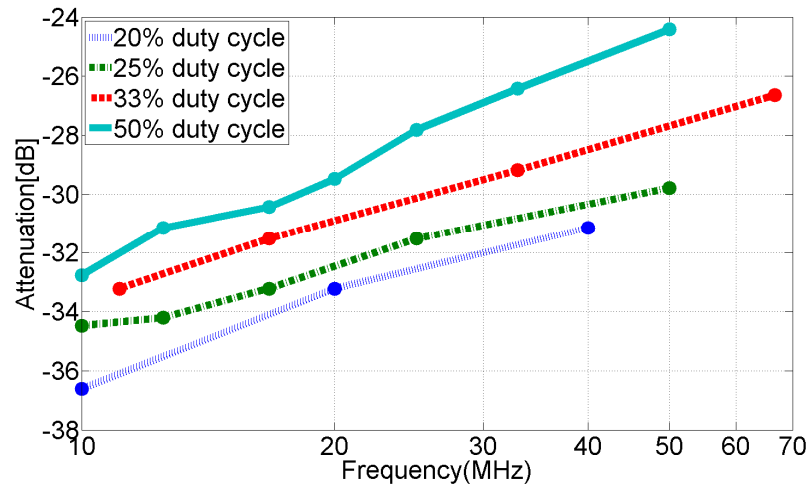


Fig. 4.4 The attenuation of signal propagated in different duty cycles generated by FPGA board

4.2.2 Pulse Occupancy for Fixed Timeslot Duration

The FPGA pulse outputs before body transmission are shown in Fig. 4.5. The plot shows a time division scheme where 1, 3, 5 and 7 timeslots are occupied when a pulse is present in those time positions of the transmitted signal. Each timeslot was set to 10 ns during the test while the pulse width was 5 ns. It should be noted, half of each timeslot were occupied by the pulses.

The graph in Fig. 4.6 shows the signal attenuation when the transmitted signal (see Fig. 4.5) has different timeslots occupancy for a fixed 8 timeslot duration (80 ns). The results show that the higher timeslot occupancy causes lower signal attenuation (around 4 dB difference between 1 and 7 occupied slots). The attenuation difference is on average 4 dB between occupied slots 1 and 5. However this decrease in attenuation was less prominent when 5 to 7 slots were increasingly occupied. The timeslot occupancy and transmission frequency both have an effect on the signal attenuation.

CHAPTER 4. EFFECT OF USER OCCUPANCY WITH BASEBAND PPM

This can be explained by the observation that higher timeslot occupancy leads to a higher transmission frequency on average. Results coincide with previous observations on signal attenuation trends for ranges of 10-100 MHz [39].

Further, the result of the female subject shows higher attenuation compared to the male subject. This could be explained by different physiological characteristics, such as the muscle mass, of the male subject arm compared to female subject. The female had less muscle and hence lower overall tissue conductivity.

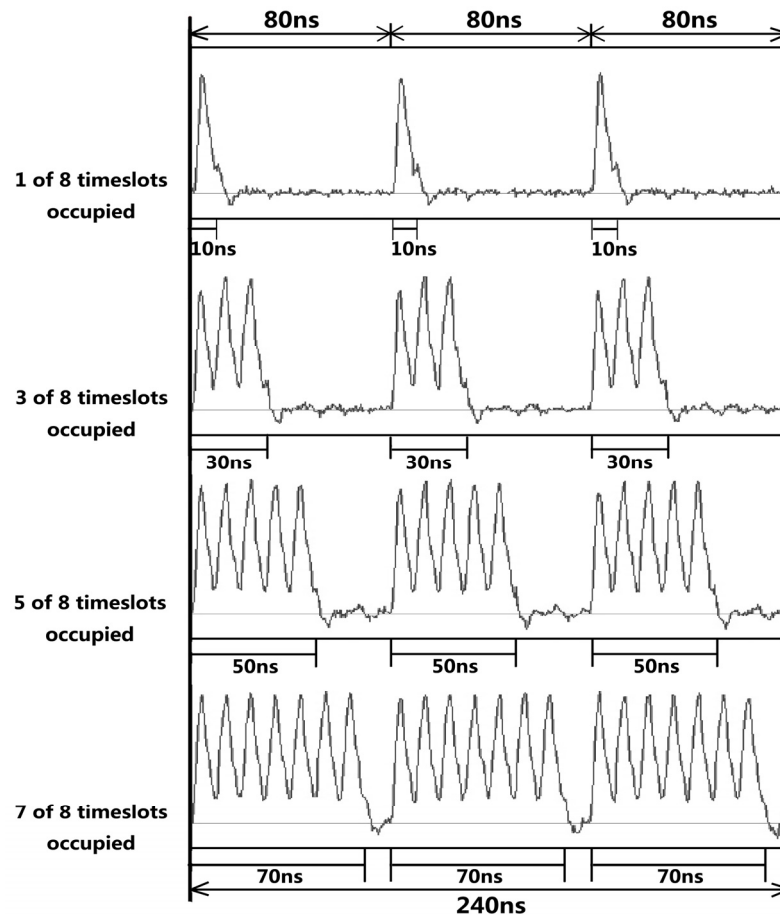


Fig. 4.5 The transmitted signal in 1, 3, 5, and 7 timeslots occupied

**CHAPTER 4. EFFECT OF USER OCCUPANCY
WITH BASEBAND PPM**

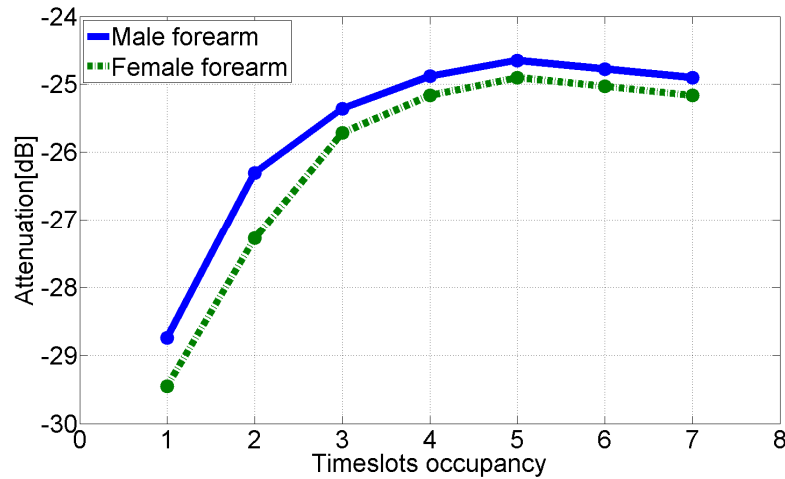


Fig. 4.6 The signal attenuation of both male and female subject forearm in 1-7 timeslots occupied using FPGA implementation

4.2.3 Pulse Occupancy for Increasing Timeslot Duration

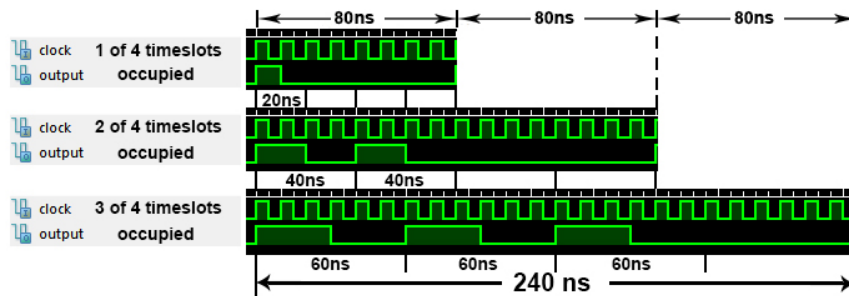


Fig. 4.7 Sample of a digital wave at 1-3 timeslots at pulse frequency of 12.5 MHz

Fig. 4.7 shows the simulated pulse shape at different timeslot occupancy (1 to 3) when the frequency was 12.5 MHz. The pulse width was variable between 10 to 30 ns during the timeslot duration was increased from 20 ns to 60 ns. Again as in the previous section (B), half of each timeslot were occupied by the pulses. Since the overall data

CHAPTER 4. EFFECT OF USER OCCUPANCY WITH BASEBAND PPM

transmission is not fully periodic, the frequency is defined as the number of pulses transmitted per second, and not the inverse of the pulse period.

In order to plot the signal attenuation of different timeslot occupancy, the FPGA transmitted three different signals as shown in Fig. 4.7 through the body. Fig. 4.8 represents the attenuation curves at frequency ranges of 5.0-25.0 MHz. Each frequency will have 1 to 3 different timeslot occupancies for attenuation comparisons. The results indicate that the body channel loss decreases when pulse occupancy increases. That is, the higher user occupancy leads to lower channel loss. For example, the calculated attenuations for different timeslots occupied at 12.5 MHz are 33.98, 29.49 and 27.14 dB, respectively.

In short, the results of the baseband digital signal transmissions indicate that for baseband digital signal transmissions, lower signal attenuations are achieved with higher user occupancies and higher pulse frequencies. There is approximately 1.0 dB

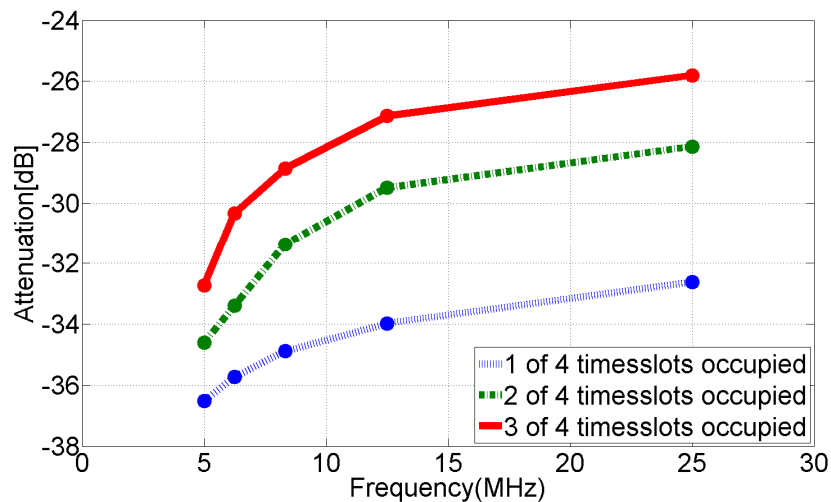


Fig. 4.8 The signal attenuation of the body forearm for 5.0-25.0 MHz in 1 to 3 timeslots occupied using FPGA implementation

CHAPTER 4. EFFECT OF USER OCCUPANCY WITH BASEBAND PPM

TABLE 4.2 The signal characteristics of body at 25 MHz

Numbers of timeslots occupied	Received signal amplitude [mV]	Attenuation [dB]
1	16.03	32.62
2	27.85	28.14
3	36.41	25.80

and 3.5 dB differences increasing from 1-3 timeslots occupied at 5.0 MHz and 25MHz, respectively. TABLE 4.2 shows the calculated signal attenuation for different timeslots occupied at 25 MHz.

4.3 Conclusion

IBC is an efficient data transmission technology for short-range transmission using human body as the communication channel. This chapter focused on the influence of timeslot occupancy and pulse duty cycle on channel loss during digital data transmission. The timeslot occupancy as one of the major factors should be considered during high data rate and low power consumption IBC transceiver design in a body area network framework. It was observed that the higher slot occupancy and pulse duty cycle provides lower signal attenuation which could be achieved by placing multiple sources on a same channel with TDM implementation. The achieved results from both FPGA (battery powered) and Pulse Generator (mains) indicates the same behavior for different duty cycles. This would help to employ efficient digital baseband signal for IBC applications.

Chapter 5

Characterization of IBC System

In this chapter, IR IBC is examined using a FPGA implementation of an IBC system. A carrier-free PPM scheme is implemented on an IBC transmitter in a FPGA board. PPM is a modulation technique which uses time based pulse characteristics to encode data and is based on impulse radio ideas. The characteristics of the proposed IBC system such as path loss, noise, SNR, and bit error rate (BER) are examined through the human body.

5.1 PPM modulation scheme

IBC realization usually employs narrow-band modulation schemes such as FSK or OOK which yield a low data rate [16][40]. In order to achieve high data rate and

CHAPTER 5. CHARACTERIZATION OF IBC SYSTEM

energy efficiency, we propose that PPM be introduced as a novel modulation mode for IBC system implementation.

PPM is one of most popular orthogonal signal modulation techniques used for both analog and digital signal transmissions. It has been widely used in WBAN communication system because of its low power consumption, transmission efficiency and anti-jamming capability. It uses pulse positions to encode the original data signal. The changes in pulse polarities in time variation due to PPM, break the regular intervals in the transmission, and therefore smoothen the overall spectrum by diminishing the line spectrum components [41]. Another reason why we employ the PPM scheme is to control the tradeoff relationship between the data rate and the reliability, namely, the BER performance.

There is a large wireless system performance improvement due to its carrierless energy efficient transmission and anti-jamming features. The wide bandwidth of PPM scheme is adequate for the IBC technique with the center frequency of 21.0 MHz [12]. The PPM scheme could be implemented without external carrier signal requirements [24]. Another advantage of using PPM is to locate the transmitted power efficiently in order to reduce the BER. For on-body wearable sensor communication, the information data are modulated by PPM and transmitted as a pulse train. Analytically, the L-PPM signal, $s(t)$, can be mathematically defined as:

$$s(t) = \sum_{k=0}^K p\left(t - b_k \frac{T}{2} - kT\right) \quad (5.1)$$

where p is the pulse waveform and T represents symbol period. It was assumed that the values of b_k for the k^{th} transmitted bit are 0 or 1.

CHAPTER 5. CHARACTERIZATION OF IBC SYSTEM

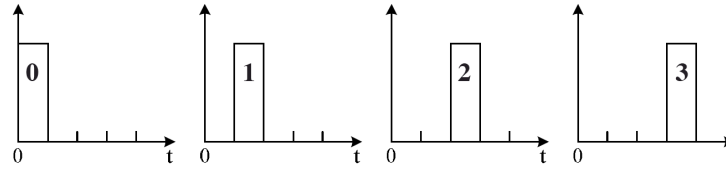


Fig. 5.1 Diagram of L=4 PPM

Fig. 5.1 describes the general structure of the 4 PPM transmitter in IBC method whereas the output of PPM transmitter is directly connected to the human body.

TABLE 5.1 Mapping of 2 bits and 3 bits words into 4 and 8 PPM symbols

4 PPM		8 PPM	
N=2	L=4	N=3	L=8
00	1000	000	00000001
01	0100	001	00000010
10	0010	010	00000100
11	0001	011	00001000
N/A		100	00010000
		101	00100000
		110	01000000
		111	10000000

In PPM technique, a binary N-bits data are mapped into one of L possible symbol positions, where $L = 2^N$. An L-bit PPM modulated signal transmitted bit information is $\log_2 L$. It is more common to share a communication channel using time division

CHAPTER 5. CHARACTERIZATION OF IBC SYSTEM

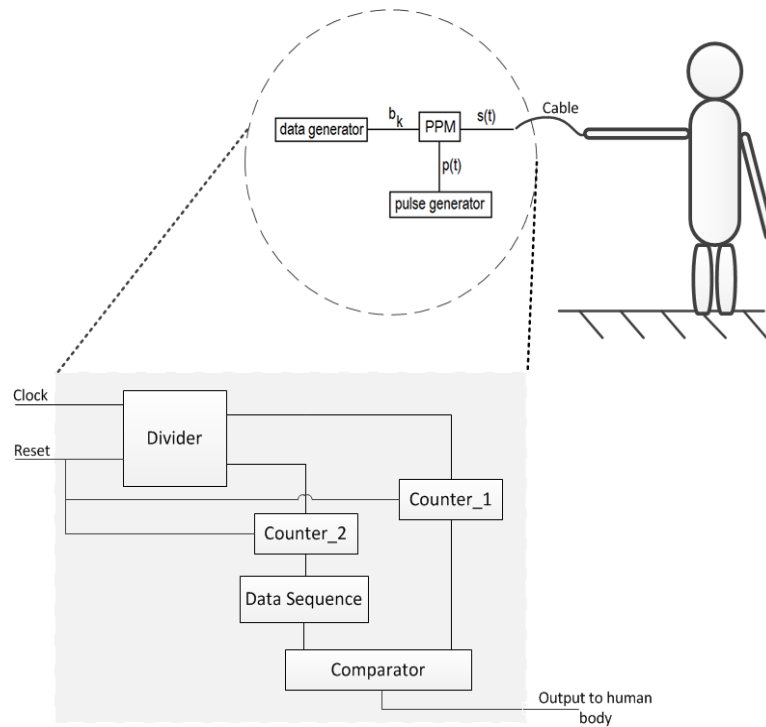


Fig. 5.2 A simplified architecture of the IBC PPM transmitter

multiplexing, where users (sensors) transmit at fixed time intervals i.e. timeslots. In a PPM timeslot, one slice is occupied by a pulse represented by each symbol and $(L-1)$ slices are empty. The data is encoded by the position of the pulse in a timeslot. TABLE 5.1 presents what we define as 4 and 8 PPM symbol modulations based on the mapping of 2 and 3 bit words, respectively.

5.2 IBC System Design

The proposed IR type of IBC PPM transmitter architecture was implemented on FPGA as shown in Fig. 5.2. This IBC transmitter circuit architecture generates a square wave

CHAPTER 5. CHARACTERIZATION OF IBC SYSTEM

digital signal for propagation through the human body. In order to have low power consumption, the design of the system requires a structure that is as simple as possible. The VHSIC (very high speed integrated circuit) hardware description language (VHDL) was employed for circuit program development.

There are five main components in our configurable architecture: a comparator, a divider, a data sequence, and two counters. The input pulse is defined as the clock frequency of FPGA board due to the carrier-free PPM scheme implementation. This clock frequency is divided by the divider component into two different frequencies based on multi-pulse position modulation requirement. These two types of frequency pulses go through both counter_1 and counter_2. Counter_1 controls timeslot distribution and Counter_2 divides each timeslot into L different slices. The following step of counter_2 is data sequence which is encoded by the pulse position represented by slice. The comparator compares the output of counter_1 and data sequence. The signal output to human body will be '1' if they are equal value; otherwise it will be '0'.

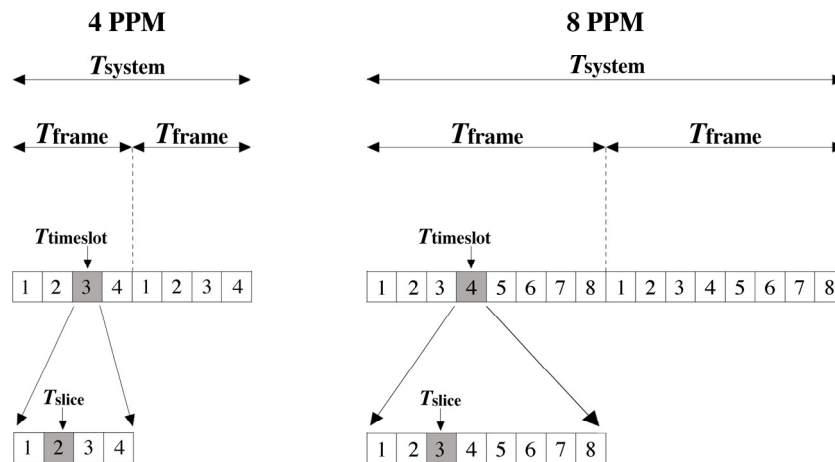


Fig. 5.3 The 4 and 8 PPM transmitter output pattern

CHAPTER 5. CHARACTERIZATION OF IBC SYSTEM

Fig. 5.3 shows the symbol period structure of proposed transmitter ($L = 4$ and 8). In a time frame for 8 PPM, it is assumed that 64 slices are transmitted. Each time frame is divided into 8 timeslots and each timeslot contains 8 time slices encoding 3 bits of data. It is worth noting that for this work, in each time slot only 1 slice out of 8 was transmitted i.e. 8 slices per frame. The clock frequency of FPGA was divided by 16 and 64 to run the counters. The position of the active slice was selected by programmable data sequence block.

5.3 Experiment setup

This work was implemented on FPGA instead of ASIC design due to its low cost high flexibility, and data rate. The proposed circuit of IBC system (see Fig. 5.4) was built on Xilinx Virtex5-XC5VLX50T FPGA Genesys board (Digilent Inc., WA). The clock frequency of FPGA board was 100 MHz and the power supply of the transmitter system was 3.3 V. The FPGA was run by battery power in order to isolate the transmitter from mains power (50 Hz) coupling effects. In the measurement setup, an oscilloscope (MSO 5204 Mixed Signal Oscilloscope, Tektronix Inc., OR) and a spectrum analyzer (NS-30, LIG-NEX1 Inc., Korea) were employed to detect the transmitted signal transmission through the body. A pair of commercial self-adhesive Ag/AgCl single electrodes (Noraxon Inc., AZ) was used as wearable transmitter and receiver electrodes. The transmitter signal amplitude was not allowed to be larger than 1 V for further safety. Although higher transmission amplitude could be the easiest way to achieve communication reliability during the experiment, it was not applied for safety reasons based on ICNIRP guideline [35]. The measured output amplitude of battery-powered FPGA was adjusted to 700 mV.

CHAPTER 5. CHARACTERIZATION OF IBC SYSTEM

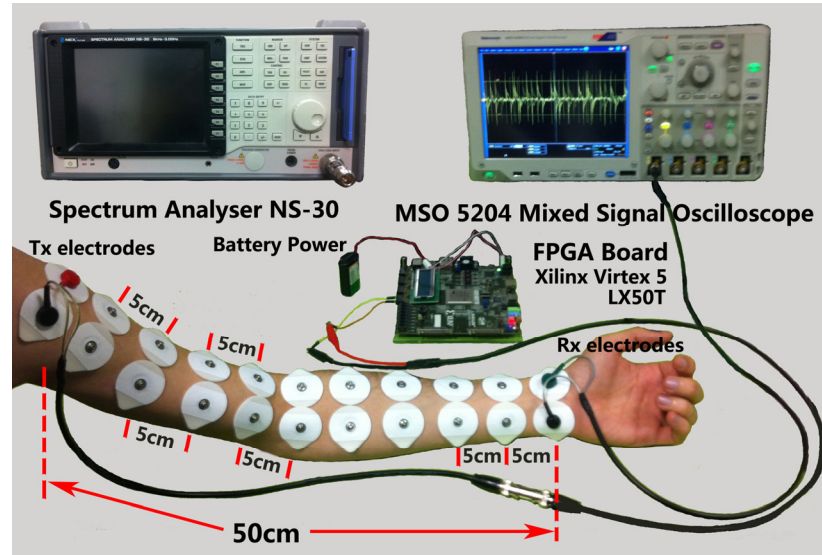


Fig. 5.4 The measurement setup and protocol of galvanic coupling IBC using FPGA board, transmitter

Two healthy male volunteers participated in the experiments. The subjects were 31 and 30 years old, 179 and 182 cm height, and 67 and 75 kg weight, respectively. In all experiments, the transmitter and receiver electrodes were attached on the subject's left arm (see Fig. 5.4). The distance between transmitter and receiver electrodes was varied from 5.0 to 50 cm. It is assumed that the human arm is composed of uniform body tissue. In fact, each 5.0 cm on-body distance between transmitter and receiver electrodes operated as a natural attenuator. We kept the receiver electrodes close to the wrist and changed the location of transmitter electrodes on the body left arm (see Fig. 5.4). The subjects were asked to stand and hold their left arm horizontally (parallel with earth ground) while the distance between arm and earth was 129 and 138 cm for both subjects, respectively.

5.4 Results and discussion

5.4.1 IBC signals (Time and Frequency domain)

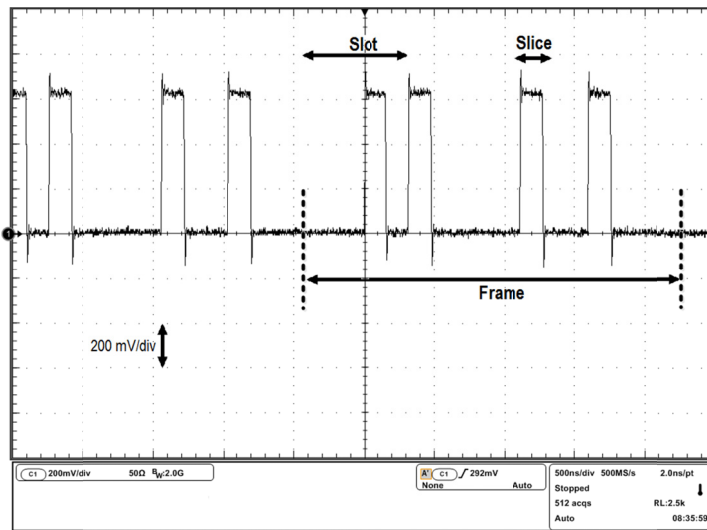


Fig. 5.5 Waveform of 4 PPM transmitter output

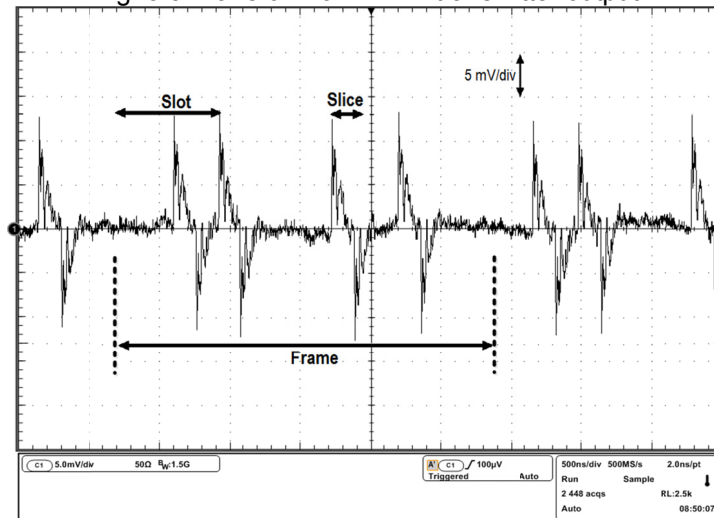


Fig. 5.6 The detected 4 PPM signal from on-body electrodes

CHAPTER 5. CHARACTERIZATION OF IBC SYSTEM

The baseband signal was modulated using 4 PPM to transmit the digital data through the body communications channel. The characteristics of IBC transmitter were measured by means of the oscilloscope. Fig. 5.5 demonstrates the waveform of a 4 PPM data sequence. The duration of each slot was 640 ns which contained four slices of 160 ns duration. Therefore, the maximum data rate of the transmitter was 1.56 Mb/s when one bit was encoded in each time slot. The voltage amplitude of transmitted 4 PPM signal was approximately 700 mV. Fig. 5.6 shows the received signal from human body which has the amplitude of 13 mV. Hence the calculated signal attenuation was around 34 dB. Additionally, the obtained results from second test subject represented the attenuation of 31.5 dB.

The baseband signal was modulated using PPM to transmit the digital data through the body communications channel. The characteristics of IBC transmitter were measured by a spectrum analyzer. Fig. 5.7 indicates the transmission power spectrum of both 4 and 8 PPM scheme. The main power of 4 PPM focused about 2.5 MHz with and the peak value of 8 PPM is around 1.5 MHz, respectively. The transmitted power value of 4 PPM is always higher than 8 PPM even at the minimum of both curves. It can be

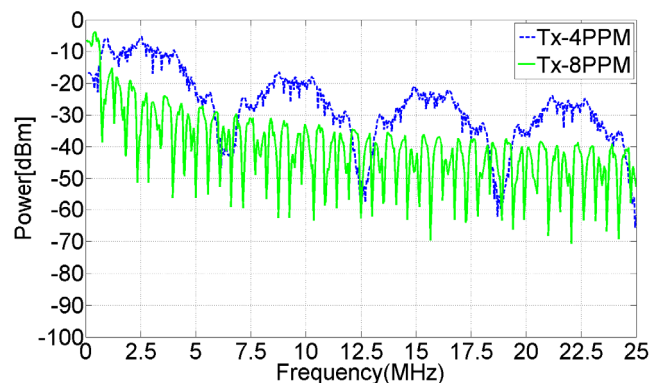


Fig. 5.7 The output signals of 4 and 8 PPM IBC transmitter (Tx) at 0-25 MHz range

CHAPTER 5. CHARACTERIZATION OF IBC SYSTEM

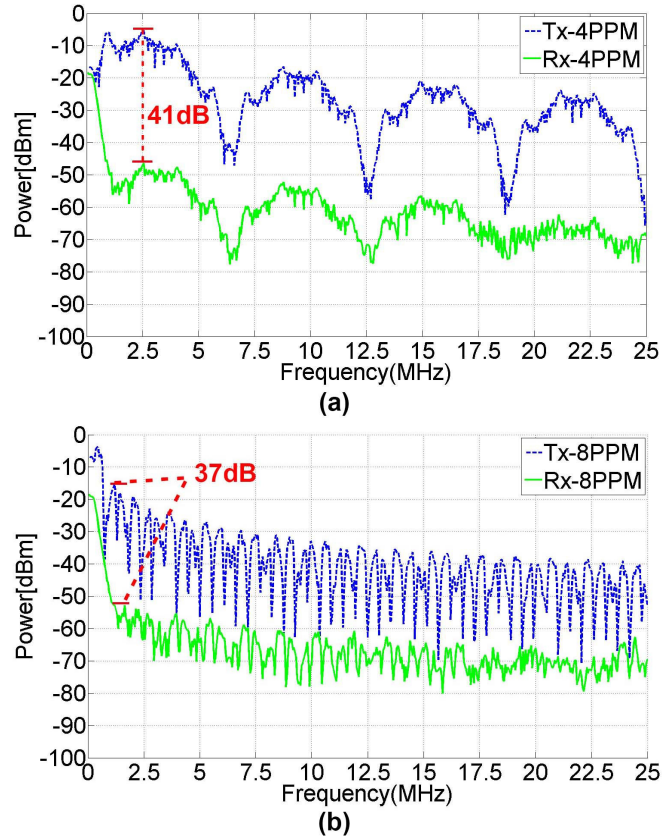


Fig. 5.8 The comparison of IBC signals spectrum, IBC transmitter (Tx) output before body and IBC receiver (Rx) output after propagating through body for (a) 4 PPM and (b) 8 PPM at 25 MHz range

clearly seen that the 4 PPM has a higher average power of approximately 15dB than 8 PPM in the 0-25 MHz frequency range.

The amplitude of signal decreased due to an increased path loss in the human body (dielectric material) propagation. Fig. 5.8 shows the comparison between the original signal and the received signal after 50 cm arm tissue transmission. There was 41 and 37 dB attenuation after 50 cm arm tissue transmission using 4 and 8 PPM scheme,

CHAPTER 5. CHARACTERIZATION OF IBC SYSTEM

respectively. The power of 4 PPM signal decreases from 6.0 to 47 dBm. And the path loss of 8 PPM signal power is between 16 and 53 dBm. Both curves start to have distortion if transmission frequency is less than 17.5 MHz. Since the signal power is weaker for detection above 17.5 MHz, the propagation bandwidth of both modulation schemes should be between 0 and 17.5 MHz which is within IEEE 802.15.6 standard range [12]. It is worth noting that the frequency spectrum of the achieved data after transmission through the body shows similar behavior with the results reported by Kobayashi *et al.* [42]. As this lower frequency range of the PPM scheme, signal is robust during investigation. It demonstrates that PPM scheme has lower attenuation and higher SNR at the operation band of IBC system.

5.4.2 Path loss characteristics

In IBC transmission system, the signal was generated by transmitter, and then propagated into the human body through the electrodes on the transmitter side. The signal is received from the electrodes on the other side. The transmitter and receiver contain electrodes instead of antennas. Hence, the power of the signal at Rx can be considered based on the Friis formula [43] and [44]:

$$P_{Rx} = P_{Tx} + G_{Tx} + G_{Rx} - P_{PL} \quad (5.2)$$

where P_{Rx} , P_{Tx} , G_{Tx} , G_{Rx} and P_{PL} are the received signal, the transmitted signal, the gain of electrodes on transmitter side, the gain of electrodes on receiver side and path loss respectively.

If path loss between the transmitted and received electrodes is modelled regarding the distance. According to an semi-empirical power decay law [45] and [46], we can express the on-body path loss as

CHAPTER 5. CHARACTERIZATION OF IBC SYSTEM

$$P_{PL}(d) = P_{PL0} + 10 n \log_{10} \left(\frac{d}{d_0} \right) \quad (5.3)$$

where d is the distance between transmitted and received electrodes along the body surface, P_{PL0} is the reference path loss at the reference distance $d_0 = 5\text{cm}$ and n is the path loss exponent which equals 2 in free space. The value of fitting coefficient n is based on the communication channel. According to [29], the value of n for on-body path loss is 1.8 on human body channel.

Moreover, the difference of the path loss between the distance d_1 and d_2 can be expressed with the following equation based on [45]:

$$\Delta P_{PLd_1}^{d_2} = P_{PLd_2} - P_{PLd_1} = 10n \log_{10} \left(\frac{d_2}{d_1} \right) \quad (5.4)$$

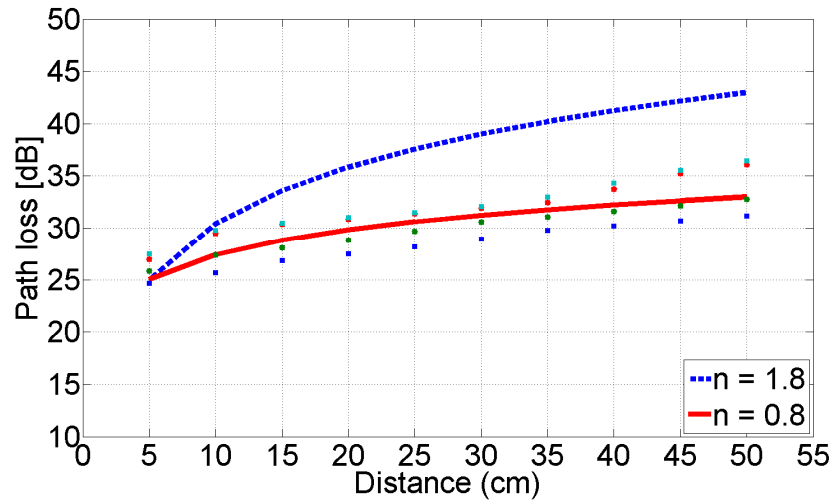


Fig. 5.9 Path loss vs distance characteristic for IBC

CHAPTER 5. CHARACTERIZATION OF IBC SYSTEM

The passloss characteristic on the human body surface was formulated based on the signal's attenuation along the body surface distance. Fig. 5.9 shows the variation of the body channel loss over the on-body channel distance. The achieved results demonstrate that the channel length enhancement led to the increase of the path loss. Our results indicated the similar behavior as mentioned by Shikada *et al.*, [19]. However, the value of on-body path loss exponent $n = 1.8$ [29] does not fit the measurement results, rather a value of $n = 0.8$ was a better fit found by Matlab software. This value is smaller than that in free space where the path loss exponent is 2.0. This finding suggests that the human body indeed acts as a transmission channel in the operation frequency band.

5.4.3 Signal propagation noise

IBC enables wireless communication without transmitting radio waves through air. Signals pass through body, hence electromagnetic noise and interference have little influence on transmissions [47]. After on-body channel, the input to the receiver is the pulse plus additive Gaussian noise [29]. To measure the amplitude of received signal and noise in our IBC system, an Oscilloscope was used. Fig. 5.10 shows the received signal after human arm transmission. As seen in the figure, the amplitude of signal is decreasing by increasing the data transmission channel distance on the body surface. At the same time, the noise remains constant.

Fig. 5.11 depicts the amplitudes of both 4 and 8 PPM received signal and measured noise, separately on the left arm. The communication distance of transmitter and receiver electrodes was varied from 5 to 50 cm). The noise amplitude curve is flat around 4 mV during various distances. Additionally, the curves of signal amplitude are linearly decreasing from 5 to 50 cm; the voltage of 4 PPM drops from 35 to 17.5

CHAPTER 5. CHARACTERIZATION OF IBC SYSTEM

mV, and the decreasing 8 PPM voltage is between 30 to 15 mV. The noise characteristics of IBC channel follow the Gaussian distribution [48] and its mean and variance values are 0 and 2.55×10^{-5} V, respectively, which is matched with the noise value of our experiment (4 mV or -15dBm).

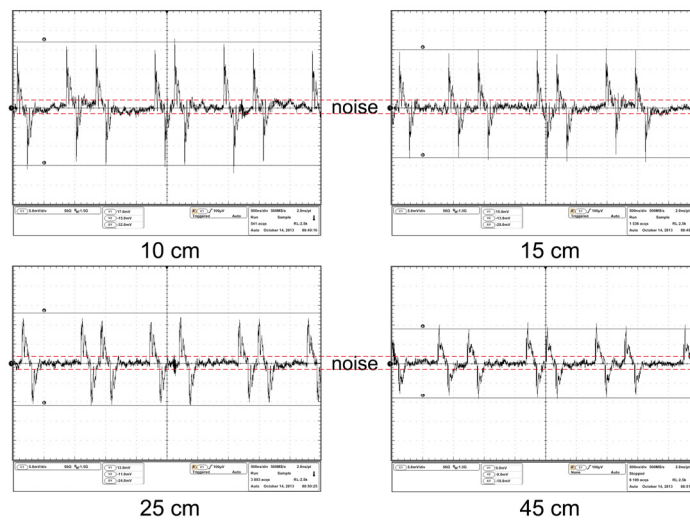


Fig. 5.10 The received signal with 10cm, 15cm, 25cm and 45cm (Tx-Rx) distance

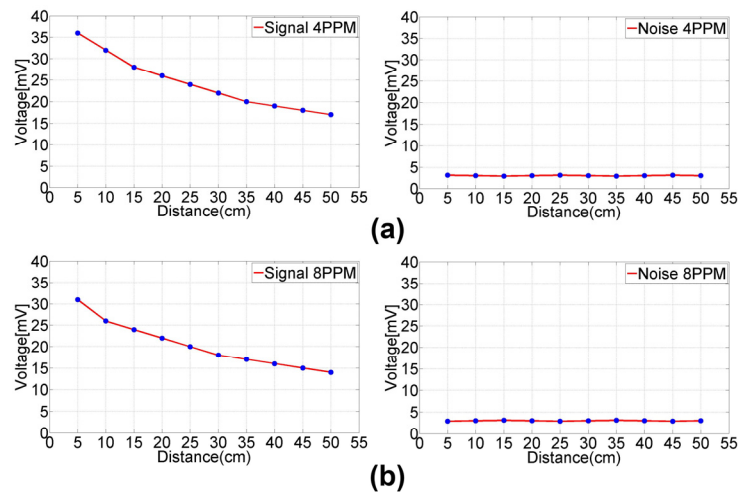


Fig. 5.11 The amplitude of IBC received signal and noise using (a) 4 PPM modulation scheme and (b) 8 PPM between 5.0 and 50 cm at human arm channel at subject-1

CHAPTER 5. CHARACTERIZATION OF IBC SYSTEM

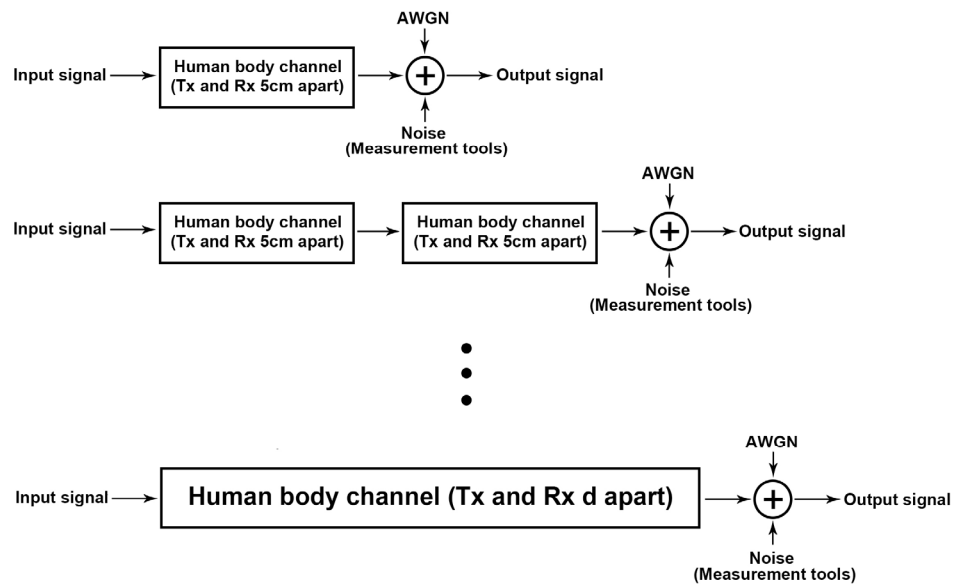


Fig. 5.12 The analytical model of the human body communication channel during different on-body channel length

To evaluate the performance of our develop system, an analytical channel model of the body channel is shown in Fig. 5.12. The human body channel distance between transmitter and receiver as well as the external noise sources are modeled. According to Wegmueller [26], we used additive white Gaussian noise (AWGN) channel model as the IBC transmission channel. As the experimental environment was similar for the IBC measurements during different channel length, the value of AWGN is supposed to be constant during the measurements.

5.4.4 Communication performance

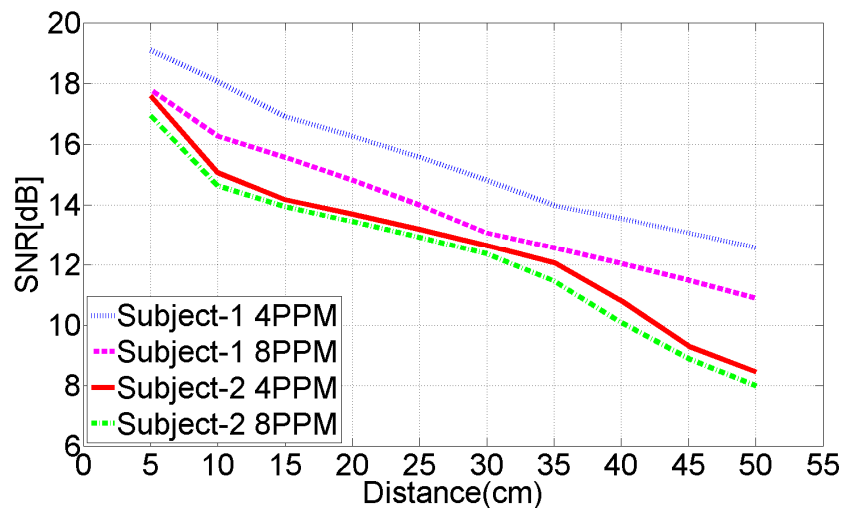


Fig. 5.13 The SNR versus channel length or distance (5-50 cm) using 4 and 8 PPM IBC system for both subject-1 and subject-2

The SNR will be calculated considering constant noise power (-15dBm). Fig. 5.13 describes the SNR variation of received signal in different distance (5-50 cm) through left arms of both subject-1 and subject-2 using 4 and 8 PPM transmission scheme. All of the 4 lines decrease almost linearly between 5 and 50 cm. The SNR are about 19 and 17.5 dB after 5cm signal propagation at subject-1 using 4 and 8 PPM scheme. If the communication distance is extended to 50cm, the SNR will be 13 and 11 dB for 4 and 8 PPM, respectively. Both subjects in the 4 PPM scheme always exhibit higher SNR than 8 PPM because of the higher average transmission frequency, see Fig. 5.8.

In both 4 and 8 PPM, subject-1 has higher SNR than subject-2, because the subject-1 arm shows lower impedance compared to subject-2 due to the ratio of muscle to fat (67 kg and 75 kg). Additionally, the difference between subject body composition

CHAPTER 5. CHARACTERIZATION OF IBC SYSTEM

creates various channel path. This explains the different SNR between subjects. For distances of 5-10 cm and 30-35 cm on those curves, there are different decreasing rates because of the effect of the joint segment. The wrist (5-10 cm) and elbow (30-35cm) present different body channel characteristics, and the arm is not entirely homogenous from end to end. Results coincide with previous observations on signal attenuation trends [49].

According to Shikada *et al.* [19], the IR type IBC transceiver has about 35dB path loss between 5 and 50 cm through body tissue. There is around 15dB attenuation from 5 to 50 cm human body channel calculated based on the receiver input power of all digital circuit wideband signaling scheme IBC system presented by Seong-Jun *et al.* [50]. In this work, SNR calculation (5-50 cm) is used to clarify the signal attenuation characteristic using PPM scheme. For subject-1, the SNR is about 6.5 dB less between 5-50 cm at both 4 and 8 PPM, there is around 8.5 dB for subject-2, respectively. Regarding the distance between transmitter and receiver electrodes, the SNR performance has rarely been reported, especially as IBC research area.

5.4.5 BER evaluation

BER is the probability that an error may occur in a bit in the pulse train where a “1” bit turns into a “0” bit or vice versa. The timeslots coding is achieved by converting each word of N bits into one of $L = 2^N$ slices for transmission. Due to the Gaussian statistics of the noise samples, the probability of error can therefore be written in terms of the error furcation. The BER for L-PPM scheme is given theoretically by [51] and [52]:

CHAPTER 5. CHARACTERIZATION OF IBC SYSTEM

$$BER_{PPM} = \frac{1}{2} \operatorname{erfc} \left(\frac{1}{2\sqrt{2}} \sqrt{\operatorname{SNR} \frac{L}{2} \log_2 L} \right) \quad (5.5)$$

where erfc is the error function:

$$\operatorname{erfc}(x) = (2\pi)^{-1/2} \int_0^{\infty} \exp(-t^2) dt \quad (5.6)$$

Fig. 5.14 shows BER performance versus IBC channel length for 4 and 8 PPM modulation scheme using theoretical simulation. Each curve is based on 10 different receiver positions on the body (see Fig. 5.5). Equation (5.6) was used to calculate the theoretical result of BER by linking the SNR to corresponding distance via the measured path loss during signal transmission through the body. As the distance between the transmitter and receiver electrodes, the BER performance reduces due to the corresponding path loss in the biological tissues. The plot shows how the BER degrades as a function of distance. For a fixed distance, the BER performance degrades from 4 PPM to 8PPM. Furthermore, as the distance increase, the BER gets worse. The similar theoretical analysis has been presented by Timmermann *et al.* [21] where their system performance evaluation of IR type transmission system was reported in terms of BER against communication distance.

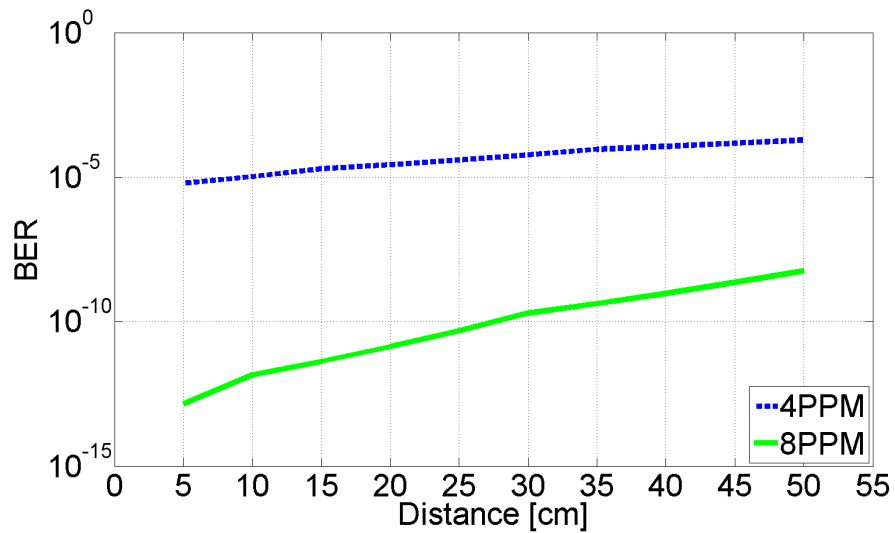


Fig. 5.14 The simulation result of BER versus distance for 4 and 8 PPM

5.5 Conclusion

This chapter presented an IBC system based on the PPM schemes for the signal transmission along the human arm. The PPM scheme (4 PPM and 8 PPM) is a novel type modulation method for IBC system design based. We examined the signal attenuation during the communication through the fixed channel lengths applying galvanic coupling IBC. The channel SNR and BER was also investigated using the implemented IBC transmitter on FPGA. Results demonstrate that around 40 dB signal attenuation after 50 cm data transmission through human arm. Additionally, the SNR decreases about 8.0 dB for a range of arm distances (5-50 cm) between transmitter and receiver electrodes with the similar amplitude of noise and various signal amplitude. Furthermore, the theoretical analysis model is established considering the human arm as a digital communication channel. The theoretically calculated BER and empirical measured SNR degrade as a function of communication channel length. The behavior

CHAPTER 5. CHARACTERIZATION OF IBC SYSTEM

of SNR as well as path loss show how signals will propagate through the human body communication channel. The proposed PPM IBC system will provide an enhanced performance for the sensor network during the biomedical applications.

Chapter 6

Conclusions and Future Work

Intrabody communications (IBC) is a novel communication technique which uses the human body itself as the signal propagation medium. This communication method is categorized as a physical layer of IEEE 802.15.6 or Wireless Body Area Network (WBAN) standard. Human body acts as a conductor for physical data transmission between wearable or implanted sensors in order to achieving low interference communication channel comparing to air. This signal transmission method attracted a lot of attention for healthcare and medical monitoring applications. Many of the design and engineering techniques that are developed for digital/analog communication, wireless mobile networks, digital processing techniques, and hardware design can be applied to the design of IBC transceivers. The low cost and power consumption IBC system is required for medical and personal healthcare need.

6.1 Thesis Summary

In this thesis, we introduced a new defined WBAN standard and the characteristics of its three different physical layers. IBC is has advantage over others and promises to be a suitable candidate for WBAN applications. After that, we demonstrated the IBC coupling methods, potential IBC modulation schemes and IBC system design. With this survey, the IBC is a potential technique for power efficiency and short distance body sensor communication networks. PPM is a suitable modulation scheme for the future IBC transmission system, because of its high SNR and low power consumption. Moreover, the international guideline of IBC safety issue is presented for the measurement setup and the electronic equipment. The basic experiment protocol is also discussed.

For the empirical study, we consider limb joint effect of human arm at IBC signal transmission for a wide frequency range (up to 200MHz). With investigation details for path loss in IBC system, our measurement results located the optimized signal transmission frequency band with low signal actuation. Also, we examined the characteristics of pulse duty cycle and timeslot occupancy through galvanic coupling IBC system. It was observed that the higher slot occupancy and pulse duty cycle provides lower signal attenuation. That would help to employ efficient digital baseband signal for IBC applications. Furthermore, we proposed a carrier-free type IBC system based on IR scheme for path loss, noise and SNR evaluation on human arm. PPM is a modulation scheme which uses time-based pulse positioning to encode data and is widely used in radio frequency IR propagations. The IR-IBC architecture based on the PPM modulation scheme was implemented on the battery powered FPGA board. The preliminary results characterize the baseband digital transmissions, in particular using PPM. This would help to develop new IBC transceiver system that

CHAPTER 6. CONCLUSIONS AND FUTURE WORK

have enhanced data rate for the medical WBAN applications compared to current IBC systems.

6.2 Challenges

IBC is a novel signal transmission method that has undergone less than 20 of years investigation by several research groups. It has recently been ratified as one of the WBAN standards. However, the lack of commercially available devices implementing this standard suggests that there are still many challenges of IBC that should be addressed.

As with all other communication systems, the data rate is pushed as high as possible for the main purpose of IBC structure design. To this end, the higher operation frequency of IBC should be determined for higher data rate. However, work should be done to determine when signals begin to radiate as RF instead of being confined to the body. The wider transmission frequency band measurement should be considered for optimal signal frequency range investigation in IBC system. There is still no previous work that exactly investigates the optimal signal transmission frequency range determination. Data throughput improvement under the low attenuation transmission frequency band is also a high priority for current and future IBC system design.

The signal duty cycle is another factor at the modulation scheme determination in IBC system design for higher data rate and power efficiency achievement. However, the signal propagation through the body on previous work was only considered based on input digital signals with 50% duty cycle. Although the average interference can be reduced by lowering pulse duty cycle [53], the signal duty cycle of IBC transmission system should be considered carefully for other duty cycles above or below 50%. In

CHAPTER 6. CONCLUSIONS AND FUTURE WORK

2010, Keisuke *et al.* [53] demonstrated that higher duty cycle signals lead to lower BER at WBAN systems. Additionally, the duty cycle optimization method is one of the major issues on energy saving of biomedical implanted communication devices [54]. It is necessary to present much more information on the characteristics based on duty cycle in the IBC channel propagation investigation.

The communication distance is one of the main features that affect the path loss of transmission channel. The quality of received signal determines the data error probability, namely BER. However, to the best of the authors' knowledge, previous work rarely presented the characteristics based on communication distance of human arm tissue in the IBC channel propagation investigation. The communication performance across channel distance is necessary to be demonstrated for different modulation schemes IBC application. The investigation of communication distance effect will raise further concerns about IBC system design.

6.3 Future work

In the future, IBC research should develop the human body channel models to describe the observed empirical results. The IBC signal propagation characteristics and communication system performance should be modeled such as path loss SNR and BER against communication distance.

Since IBC transmitter has been employed in our system, the IBC receiver design should be another remaining challenge. PPM transmission system should be paid much more attention because of its communication performance. Furthermore, we should focus on IR type IBC system on chip design, layout and fabrication. The future developed IBC system will be the main part of wireless portable monitoring network

CHAPTER 6. CONCLUSIONS AND FUTURE WORK

system. It will provide better patient convenience and results in further development of low cost sensors networks around the human body.

References

- [1] K. A. Mark, "The Critical Care Crisis in the United States A Report From the Profession." in *CHEST Journal*, vol. 125, no. 4 , pp. 1514-1517,2004.
- [2] A. Dhamdhere, H. Chen, A. Kurusingal, V. Sivaraman, and A. Burdett, "Experiments with wireless sensor networks for real-time athlete monitoring," in *IEEE Local Computer Networks (LCN)*, Oct. 2010, pp. 938–945.
- [3] B. Schrick and M. J. Riezenman, *Wireless Broadband in a box*, [Online] Available :http://oldeee.see.ed.ac.uk/private/ee4/Org09-10/wireless_broad.pdf, 2012.
- [4] M. Paksuniemi, H. Sorvoja, A. Alasaarela, and R. Myllyla, "Wireless sensor and data transmission needs and technologies for patient monitoring" in *the operating room and intensive care unit, EMBC*, Shanghai, China, 2005, pp. 5182–5185.

REFERENCES

- [5] J. Bae, “a Low Energy Wireless Body Area Network Transceiver with scalable Double FSK Modulation,” Ph.D. dissertation, KAIST, Korea, 2012.
- [6] *Wireless Body Area Network: Seminar Report and PPT*, [Online] Available :<http://www.seminaronly.com/computer%20science/wireless-body-area-network.php>, 2013.
- [7] *IEEE 802.15*, [Online] Available : http://en.wikipedia.org/wiki/IEEE_802.15, 2014.
- [8] *Testing BAN (WBAN) Networks and IEEE 802.15.6*, [Online] Available : <http://www.ni.com/white-paper/14285/en/>, 2014.
- [9] M. Patel and J. Wang, “Applications, challenges, and prospective in emerging body area networking technologies,” *IEEE Commun. Magazine*, vol. 17, no. 1, pp. 80–88, Feb. 2010.
- [10] S. Adibi, “Link technologies and blackberry mobile health (mhealth) solutions: A review,” *IEEE Trans. Inf. Technol. Biomed.*, vol. 16, no. 4, pp. 586–597, Jul. 2012.
- [11] M. Lauzier, P. Ferrand, H. Parvery, A. Fraboulet, and J.-M. Gorce, “WBANs for live sport monitoring: An experimental approach, early results and perspectives,” in *EURO-COST IC1004*, Sep. 2012, pp. 1–6.

REFERENCES

- [12]“IEEE Standard for Local and metropolitan area networks Part 15.6: Wireless Body Area Networks,” *IEEE Std. 802.15.6-2012*, pp. 1-271, 2012.
- [13]J. Wang and Q. Wang, *Body Area Communications: Channel Modeling, Communication Systems, and EMC*. Singapore : Wiley (Asia), 2013.
- [14]H. J. Yoo, “Wireless body area network and its healthcare applications,” in *IEEE Asia-Pacific Microwave Conf. (APMC’13)*, Nov. 2013, pp. 89–91.
- [15]P. Arun, “Architecture for ultra-low power multi-channel transmitters for Body Area Networks using RF resonators,” PH.D. dissertation, Massachusetts Institute of Technology, USA, 2011.
- [16]B. Joonsung, S. Kiseok, L. Hyungwoo, C. Hyunwoo, and Y. Hoi-Jun, “A low-energy crystal-less double-FSK sensor node transceiver for wireless body-area network,” *Solid-State Circuits, IEEE Journal*, vol. 47, pp. 2678-2692, 2012.
- [17]T. G. Zimmerman, “Personal area networks: near-field intrabody communication,” *IBM systems Journal*, vol. 35, pp. 609-617, 1996.

REFERENCES

- [18] C. Steven, A. Argyriou, Z. W. Bhatti, and H. Baldus, "A Body-Coupled Communication and Radio Frequency Dual Technology Cooperation Protocol for Body-Area Networks," status: published, 2010.
- [19] K. Shikada and W. Jianqing, "Development of human body communication transceiver based on impulse radio scheme," in *CPMT Symposium Japan*, 2012 2nd IEEE, 2012, pp. 1-4.
- [20] M. Seyedi, B. Kibret, D. T. H. Lai, and M. Faulkner, "A survey on intrabody communications for body area network applications," *Biomedical Engineering, IEEE Transactions*, vol. 60, pp. 2067-2079, 2013.
- [21] J. Timmermann, E. Pancera, G. Adamiuk, W. Wiesbeck, and T. Zwick, "Estimated performance of UWB impulse radio transmission including dirty RF effects," in *Ultra-Wideband, ICUWB. IEEE International Conference*, 2008, pp. 205-208.
- [22] V. Niemela, M. Hamalainen, and J. Iinatti, "On IEEE 802.15.6 UWB symbol length for energy detector receivers' performance with OOK and PPM," in *Medical Information and Communication Technology (ISMICT)*, 2013 7th International Symposium on, 2013, pp. 33-37.

REFERENCES

- [23] A. N. Kim, P. A. Floor, T. A. Ramstad, and I. Balasingham
“Communication using ultra wide-band pulse position modulation for
in-body sensors,” in *7th IEEE/ACM Body Area Networks Conference
(Bodynets)* 2012, pp. 159-165.
- [24] X. Fu, G. Chen, T. Tang, Y. Zhao, P. Wang, and Y. Zhang, “Research and
simulation of PPM modulation and demodulation system on spatial
wireless optical communication,” in *Photonics and Optoelectronic
(SOPO)*, 2010, pp. 1-5.
- [25] S. Da-shan, and J. M. Kahn. "Differential pulse-position modulation for
power-efficient optical communication." *Communications, IEEE
Transactions*, vol. 47, no. 8, pp. 1201-1210, 1999.
- [26] M. S. Wegmueller, “Intra-Body Communication for Biomedical Sensor
Networks,” Ph.D. dissertation, ETH Zurich, Switzerland, 2007.
- [27] K. Hachisuka, A. Nakata, T. Takeda, Y. Terauchi, K. Shiba, K. Sasaki, H.
Hosaka, and K. Itao, “Development and performance analysis of an
intra-bodycommunication device,” In *Solid-State Sensors, Actuators and
Microsystems, 12th International Conference*, 2003, vol. 2, pp. 1722-1725.
- [28] M. Wegmueller, A. Lehnert, J. F. R. Reutemann, M. Oberle, N. Felber, N.
Kuster, O. Hess, and W. Fichtner, “Measurement system for the

REFERENCES

- characterization of the human body as a communication channel at low frequency,” in *27th Annual International Conference Engineering in Medicine and Biology Society*, 2005, pp. 3502-3505.
- [29]J. Shi, and J. Wang. "Dual-mode impulse radio ultra-wideband transmission for body area networks." *IET microwaves, antennas & propagation*, vol. 5, no. 10, pp. 1250-1255, 2011.
- [30]T. Leng, Z. Nie, W. Wang, F. Guan and L. Wang, "A human body communication transceiver based on on-off keying modulation," *Bioelectronics and Bioinformatics (ISBB), 2011 International Symposium on* , vol., no., pp.61,64, 3-5 Nov. 2011.
- [31]K. Katsu, D. Anzai, and J. Wang. "Performance evaluation on correlation detection and energy detection for ultra wideband-impulse radio communication with multi-pulse position modulation scheme in implant body area networks." *IET Communications*, vol. 7, no. 13, pp. 1430-1436, 2013.
- [32]D. Anzai K. Katsu, R. Chavez-Santiago, Q. Wang, D. Plettemeier; J. Wang and I. Balasingham, "Experimental Evaluation of Implant UWB-IR Transmission With Living Animal for Body Area Networks," *Microwave*

REFERENCES

- Theory and Techniques, IEEE Transactions on* , vol.62, no.1, pp.183,192, Jan. 2014.
- [33]S. Gabriel, R. Lau, and C. Gabriel, “The dielectric properties of biological tissues: Iii. parametric models for the dielectric spectrum of tissues,” *Phys. Med. Biol.*, vol. 41, no. 11, pp. 2271–2293, Nov. 1996.
- [34]J. Bae, K. Song, H. Lee, H. Cho, and H.-J. Yoo, “A low-energy crystal-less double-FSK sensor node transceiver for wireless body-area network,” *IEEE J.Solid-State Circuits*, vol. 47, no. 11, pp. 2678–2692, Nov. 2012.
- [35]International Commission on Non-Ionizing Radiation Protection (ICNIRP), “Guidance for limiting exposure to time-varying electric, magnetic, and electromagnetic fields (up to 300 GHz),” *Health Physics*, vol. 74, no. 4, pp. 494–522, Apr. 1998.
- [36]S. MirHojjat and D. T. H. Lai. "Effect of Limb Joints and Limb Movement on Intrabody Communications for Body Area Network Applications." *Journal of Medical and Biological Engineering*, vol. 34, no. 3, 2014.
- [37]M. Seyedi, B. Kibret, D. T. H. Lai, and M. Faulkner, "An empirical comparison of limb joint effects on capacitive and galvanic coupled

REFERENCES

- intra-body communications," in *Intelligent Sensors, Sensor Networks and Information Processing, 2013 IEEE Eighth International Conference*, 2013, pp. 213-218.
- [38][Online]. Available :
<http://www.minicircuits.com/MCLStore?MedelInfoDisplay>.,2013.
- [39]M. Callejon, D. Naranjo-Hernandez, J. Reina-Tosina, and L. Roa, "A comprehensive study into intra-body communications measurements," *IEEE Trans. Instrum. Meas.*, vol. 62, pp. 2446–2455, 2013.
- [40]L. Tengfei, N. Zedong, W. Wenchen, G. Feng, and W. Lei, "A human body communication transceiver based on on-off keying modulation," in *Bioelectronics and Bioinformatics (ISBB), 2011 International Symposium*, 2011, pp. 61-64.
- [41]M. Hämäläinen, *Singleband UWB Systems: Analysis and Measurements of Coexistence with Selected Existing Radio Systems*, University of Oulu, 2006.
- [42]T. Kobayashi, Y. Shimatani, and M. Kyoso. "Application of Near-field intra-body communication and spread spectrum technique to vital-sign monitor." In *Engineering in Medicine and Biology Society (EMBC), 2012* pp. 4517-4520.

REFERENCES

- [43] *Friis transmission equation*, [Online] available:
http://en.wikipedia.org/wiki/Friis_transmission_equation
- [44] T. V. Pham, Y. T. Kim, M. T. L. Thi, and H. A. Tuy, "An empirical channel model for Human Body Communication," in *Advanced Technologies for Communications (ATC), 2010 International Conference*, 2010, vol. 352, no. 355, pp. 20-22.
- [45] Y. Ai, We. Tao, and C. Choy, "A simulation-oriented channel modeling methodology for human on-body channel communication," in *Emerging Applications of Information Technology (EAIT), 2012 Third International Conference*, pp. 73-76, 2012.
- [46] H.A. Rahim, F. Malek, A. I. Ahmad, and M. F. A. Malek. "Path Loss Characterization of Body-to-body Radio Propagation Channel on the Angular Variations." *Session IPK*: 399.
- [47] H. Zhu, R. Xu, and Jie Yuan, "High speed intra-body communication for personal health care," Engineering in Medicine and Biology Society, 2009. EMBC 2009. Annual International Conference of the IEEE , vol., no., pp.709,712, 3-6 Sept. 2009

REFERENCES

- [48] T. Kobayashi, C. Sugimoto, and R. Kohno, "Performance evaluation of the spread spectrum human body communication devices," in *Medical Information and Communication Technology (ISMICT)*, 2014, pp. 2-4.
- [49] M. Seyedi, D. T. H. Lai, and M. Faulkner, "Limb joint effects on signal transmission in capacitive coupled intra-body communication systems," in *Engineering in Medicine and Biology Society (EMBC)*, 2012 Annual International Conference of the IEEE, 2012, pp. 6699-6702.
- [50] S. Seong-Jun, C. Namjun, K. Sunyoung, and Y. Hoi-Jun, "Energy-efficient human body communication receiver chipset using wideband signaling scheme," in *Engineering in Medicine and Biology Society (EMBS)*, 2007, pp. 2292-2295.
- [51] T. Y. Elgarni, "Performance Comparison between OOK, PPM and PAM Modulation Schemes for Free Space Optical (FSO) Communication Systems: Analytical Study," *International Journal of Computer Applications*, vol. 79, no. 11, pp. 0975 – 8887, 2013.
- [52] V. Manea, R. Dragomir, and S. Puscoci, "OOK and PPM modulations effects on bit error rate in terrestrial laser transmissions," in *telecommunication conference*, pp. 55-61, 2011.

REFERENCES

- [53]S. Keisuke, K. Ishibashi, and R. Kohno, “An analysis of interference mitigation capability of low duty-cycle UWB communications in the presence of wideband OFDM system,” *Wireless personal communications*, vol. 54, pp. 39-52, 2010.
- [54]Z. Xu and Y. Li. “Energy-constrained duty-cycle optimization for wireless implanted communication devices,” *E-Health Telecommunication Systems and Networks*, vol. 1, pp. 6-11, 2012.